



# **Resource-efficient fuel additives for reducing ash related operational problems in waste wood combustion (REFAWOOD)**

## **Joint final report of the project**

**Zeng, Thomas (DBFZ)**

**Hamberger, Andreas (Endress)**

**Heese, Markus (Endress)**

Gefördert durch:



aufgrund eines Beschlusses  
des Deutschen Bundestages

The project on which this report is based was funded by the Federal Ministry of Food and Agriculture (BMEL) through the Fachagentur Nachwachsende Rohstoffe e.V. (Agency for Renewable Resources) – the executing agency of the BMEL for the Renewable Resources Promotion Programme – on the basis of a resolution of the German Bundestag. The author is responsible for the content of this publication.

DBFZ Deutsches Biomasseforschungszentrum gemeinnützige GmbH  
Torgauer Straße 116  
D-04347 Leipzig

Tel. + 49-341-2434-112  
Fax + 49-341-2434-133  
eMail: [info@dbfz.de](mailto:info@dbfz.de)

Date: 01.08.2019



Funding agency	Fachagentur Nachwachsende Rohstoffe e. V. (FNR) Dr.-Ing. Andrej Stanev Hofplatz 1 18276 Gülzow-Prüzen Germany
Contact Sub-project 1	DBFZ Deutsches Biomasseforschungszentrum gemeinnützige GmbH Torgauer Straße 116 04347 Leipzig Germany Tel.: +49 (0)341 2434-112 Fax: +49 (0)341 2434-133 Email: <a href="mailto:info@dbfz.de">info@dbfz.de</a> Web: <a href="http://www.dbfz.de">www.dbfz.de</a> <b>Dipl.-Ing. Thomas Zeng</b> Tel.: +49 (0)341 2434-542 Fax: +49 (0)341 2434-133 Email: <a href="mailto:thomas.zeng@dbfz.de">thomas.zeng@dbfz.de</a>
Contact Sub-project 2	ENDRESS Holzfeuerungsanlagen GmbH Industriestraße 18 91593 Burgbernheim Germany Tel.: +49 (0) 9843 93 63 48 – 0 Fax: +49 (0) 98 43 93 63 48 – 22 Email: <a href="mailto:info@endress-feuerungen.de">info@endress-feuerungen.de</a> Web: <a href="http://www.endress-feuerungen.de">www.endress-feuerungen.de</a> <b>Markus Heese (Geschäftsführer)</b> Email: <a href="mailto:markus.heese@endress-feuerungen.de">markus.heese@endress-feuerungen.de</a>
Creation date:	01 August 2019
Project number funding agency:	22404215 (sub-project 1, DBFZ) 22404315 (sub-project 2, Endress)
Duration	01 April 2016 – 31 March 2019
Total number of pages	52

## Table of contents

<b>I.</b>	<b>Aims.....</b>	<b>5</b>
<b>1</b>	<b>Task .....</b>	<b>5</b>
<b>2</b>	<b>State of the art.....</b>	<b>6</b>
<b>3</b>	<b>Cooperation with other bodies .....</b>	<b>10</b>
<b>II.</b>	<b>Results.....</b>	<b>10</b>
<b>1</b>	<b>Materials and methods.....</b>	<b>11</b>
<b>1.1</b>	Raw material procurement and fuel production .....	11
<b>1.2</b>	Combustion tests on a pilot plant scale .....	15
<b>1.3</b>	Industrial-scale combustion tests .....	16
<b>1.4</b>	Fuel and ash analysis .....	21
<b>2</b>	<b>Achieved results .....</b>	<b>22</b>
<b>2.1</b>	Fuel production.....	22
<b>2.2</b>	Combustion tests on a pilot plant scale .....	25
<b>2.3</b>	Industrial-scale combustion tests .....	30
	2.3.1 Implementation of additive dosing .....	30
	2.3.2 Combustion tests .....	32
<b>2.4</b>	Conclusions.....	41
<b>3</b>	<b>Knowledge from third parties.....</b>	<b>41</b>
	<b>References .....</b>	<b>43</b>

## List of abbreviations and symbols

Abbreviations	Explanation
WP	work package
bld	below limit of detection
G	recycled gypsum
H	halloysite
CHP	cogeneration of heat and power
LCA	life cycle assessment
WCB	residues from chipboard processing
WLR	wood logging residues
XRD	X-ray diffraction

## I. Aims

### 1 Task

The energetic use of residual and used wood is becoming increasingly important. Against the background of restrictive landfill regulations and rising prices for untreated wood assortments, especially in Germany and Sweden, there is also a trend that the energy markets, which are characterized by fluctuating electricity supply from renewable energy sources, are to be stabilized by flexible CHP plants. Since these plants are increasingly designed for a range of different fuels, inexpensive fuels are of interest for economical operation, i.e. fuels such as the above-mentioned residual and used wood resulting from residual material and waste streams. However, these fuel ranges can lead to problems in plant operation due to critical constituents. The main problem areas are the increased risk of slagging and the deposits on the exhaust side, e.g. on the heat exchanger surfaces. These have a negative influence on the heat transfer and lead to a reduction in the service life of the plant due to the corrosion processes associated with the deposits. These problems are known in almost all biomass and used wood-fired power plants. Thus, the use of low-cost biomass fuel ranges requires not only adapted supply chains but also the use of appropriate conversion plants and exhaust gas purification technologies. Therefore, when operating biomass (heating) power plants, the savings in fuel costs must always be weighed against the higher costs for plant technology and operation.

The fuel properties of inexpensive biomass ranges can be considerably improved by the use of suitable additives. Various additives were successfully tested both for reducing the risk of slagging and for reducing deposits on the exhaust side [1–3]. Nevertheless, there is still a considerable need for research and development. In particular, the identification of inexpensive and resource-efficient additives and their testing on an industrial scale require increased efforts. The resulting increase in the use of residual and waste biomass reduces dependence on fossil fuels. The additives should be characterized by high flexibility, reactivity and stability and should also be available in large quantities at low cost, e.g. due to a high volume of waste streams.

The overall objective of the Era-Net Refawood project was to increase the efficiency and sustainability of the use of residual and used wood in CHP plants by using resource-efficient additives. The approach in the Refawood project was based on the combination of basic research, applied research and the transfer of findings into experiments in large-scale industrial plants. By using, for example, inexpensive recycled gypsum materials as additives, possibilities are identified and opened up to increase the economic efficiency and sustainability of the use of used wood in cogeneration plants. The following objectives were pursued in detail:

- Proposal of an efficient and innovative fuel additive concept to reduce the problems arising from the use of inferior wood assortments in the operation of combustion plants (ash deposits, corrosion, slagging of the combustion chamber ash),
- proof of the effectiveness of the fuel additive concept on an industrial scale,

- the application of the fuel additive concept in order to enable environmentally friendly, resource-saving and economical operation of power plants,
- determination of possible savings in operating and maintenance costs through the application of the fuel additive concept,
- development of recycling concepts and application options for the ashes of used wood combustion,
- determination of the influence of various additives on the environmental balance and economy of heating plants and combined heat and power plants.

## 2 State of the art

In the research project presented here, novel additives were used in the combustion of residual and used wood in order to reduce problems in the operation of combustion plants. In the following, the current state of the art in science and technology is briefly presented. Due to the challenges of the use of residual and used wood as well as non woody biomass in the combustion process, the use of residual and used wood in the heating sector has so far been rather low and is justified, among other things, by [4]:

- the comparatively problematic fuel properties,
- a combustion or complete plant technology with limited availability, which can be used to ensure compliance with the statutory environmental protection requirements, and
- the currently strongly fluctuating price situation.

As with all thermochemical conversion processes used to generate energy, the priority objectives for the use of residual and used wood in combustion plants can be summarized as follows:

- high plant efficiency,
- low-emission combustion,
- high system availability and
- lower maintenance effort.

The difficulty in achieving high plant efficiency, low-emission combustion and high plant availability is in particular due to the sometimes problematic composition of residual and used wood and the resulting effects on combustion. Since these problems do not only occur with residual and used wood and, in addition, only a limited number of publications deal exclusively with these inferior wood assortments, the relationships between fuel properties and composition as well as combustion and emission behavior in general are described in the following on the basis of difficult biomass fuels.

### Emissions

A distinction is made between products of complete ( $H_2O$  and  $CO_2$ ) and incomplete combustion ( $CO$ , hydrocarbons), in-situ formed pollutants (PCDD/PCDF, VOC) and products of various fuel components ( $NO_x$ ,  $SO_2$ ,  $HCl$ , etc.). In addition, particulate matter is formed [5]. Non-woody biomass fuels or low-

quality wood fuels have typically higher contents of nitrogen, silicon, sulphur, chlorine and alkali metals such as sodium and potassium compared to clean wood [6–8]. These elements are partially released during the combustion process and, under stable combustion conditions and a complete gas phase burnout, are the cause for the formation of gaseous emissions, sulphur oxides ( $\text{SO}_2$ ) and HCl, as well as for particulate matter emissions. In addition to the emissions mentioned above, these elements also cause a high sintering and slagging tendency of the ash, which in turn lead to problems in the combustion process. Therefore, the combustion of non woody biomass is technically demanding and requires the consideration of a large number of individual processes [4, 9, 10].

In particular, the formation mechanisms of gaseous  $\text{SO}_2$  and HCl, which are directly related to the mineral behavior in the fuel in addition to the sulphur and chlorine content in the fuel [4, 9–11]. During combustion, sulphur and chlorine from the fuel mainly form gaseous emissions ( $\text{SO}_2$  and HCl) as well as alkali or alkaline earth chlorides or sulphates, which are emitted as fine dust or remain in the bottom ash. Studies with straw show, for example, retention rates of 40 - 80 % of the sulphur in the bottom ash [12]. This retention seems to be directly related to the amount of calcium in the fuel to form  $\text{CaSO}_4$  [4, 9, 10] and is used e.g. by using calcium-containing additives to reduce emissions. This was investigated by different authors [13–16]. The exact mechanism can be found in Obernberger et al. [10] and Christensen et al. [17]. Compared to sulphur, the retention rate of chlorine in the bottom ash is much lower, i.e. less than 20 % [17] since a large proportion is emitted as HCl or in the form of volatile salts as particulate matter. In addition to the molar ratio of sulphur to chlorine (2S/Cl ratio), this distribution of chlorine is essentially dependent on the presence of other minerals such as potassium, calcium and silicon. By the formation of potassium and calcium chlorides a reduction of the gaseous HCl in the combustion is possible, which is used by additive addition [13–15]. In contrast, the presence of silicon in the fuel favors the formation of potassium silicates, which reduces both chlorine and sulphur retention in the bottom ash [15, 16]. Further investigations by Knudsen et al. also show that the integration of sulphur and chlorine is influenced not only by the mineral composition but also by the decomposition temperature of the biomass [12].

In addition to gaseous emissions, fine dust particles are formed and released. The term fine dust or ultrafine particles describes a complex mixture of solid and/or liquid organic and inorganic pollutants discharged into the air, which vary according to size, composition and origin and are described by particle size or aerodynamic diameter [9]. The formation of particulate emissions during complete combustion is directly related to the fuel composition. The main components of fine dusts are:

- low-volatile mineral ash components (e.g.  $\text{CaO}$ ,  $\text{Al}_2\text{O}_3$ ,  $\text{SiO}_2$ ) which are carried along by the combustion air, and
- ash compounds (aerosols) which are formed by evaporation and condensation or new formation in the furnace (e.g.  $\text{KCl}$ ,  $\text{K}_2\text{SO}_4$ , nitrates).

The entrainment of low-volatile mineral ash constituents predominantly leads to the formation of fly ash with a particle size between 10 and 100  $\mu\text{m}$ . In small combustion appliances (<100 kW) at least 80 - 90% of the particulate matter is characterized by a particle size below 1  $\mu\text{m}$  (< PM<sub>1</sub>), which are called aerosols [4, 9, 12, 17, 18]. For non-woody biomass fuels, K, Na, S, Cl and possibly P are the main causes of dust emissions, as these evaporate to a large extent during the combustion process and then form new particles by nucleation or condense on existing ones [19–25]. Further components such as Zn and Pb accumulate on existing particles through secondary condensation processes. According to Sommersacher et al., the sum parameter (K, Na, Zn, Pb) can be used to estimate the emission of PM<sub>1</sub> [11]. Three fuel classes were used to show that fine dust emissions increase with

increasing sum parameters. For fuels with a high phosphorus content (e.g. fermentation residues, rape press cake), phosphorus also contributes significantly to the formation of particulate matter [13, 26].

The potassium compounds formed by condensation can account for a large proportion of particle emissions during complete combustion. Depending on the temperature in the firebed, they occur mainly in the form of potassium chloride (KCl), potassium sulphate ( $K_2SO_4$ ), potassium hydroxide (KOH) and potassium carbonate ( $K_2CO_3$ ). There are a number of studies on the temperature dependence of the release of potassium compounds [12, 26–28]. Interactions with other mineral fuel components can have a strong influence on the volatility of potassium [5, 12]. As a result, they play a key role in reducing particulate matter emissions. Several working groups have evaluated the possibilities of correlating the amount of particulate matter and various sum parameters for ash rich fuels. In his studies on the combustion of oats, peat and rapeseed press cake, Tissari found that the relatively small increase in fine dust emissions could be attributed to higher S/Cl, S/K and K/Cl ratios in the fuel, despite the significantly higher ash content compared with wood fuels [26]. It is assumed that the high sulphur content causes the sulphation of potassium, whereby  $K_2SO_4$  is less volatile than KCl and thus prefers to remain in the grate ash during the temperature interval under consideration. This work thus confirms earlier studies on the formation of fine dust when biomass is used in fixed-bed furnaces [12, 16, 29]. The dependence of the formed potassium species in the particulate matter on certain sum parameters in the fuel was investigated. It was shown that especially the ratios  $(2S+Cl)/(K+Na)$  and  $2S/Cl$  allow statements on whether potassium is preferably released as chloride or sulphate or whether more carbonates, hydroxides and oxides are formed. Knudsen et al. investigated the influence of the silicon content on the release of potassium from ash-rich biomass fuels (rice, barley, wheat, oats, mustard, rape) [12]. This showed that a low K/Si ratio in the fuel can reduce the release of potassium and thus the formation of particulate matter. This is also confirmed by recent investigations by Sommersacher et. al. [11]. However, a high Cl/K ratio can mask this effect, so that even with a low K/Si ratio potassium is preferably released as KCl and not bound in the ash.

The interactions of potassium with other minerals can also be used specifically to reduce particulate matter emissions. This includes the use of mineral additives or mixing with other raw materials of suitable composition. Kaolin has proven to reduce particulate matter, which leads to the integration of potassium into the aluminium silicate structure [13, 14, 30–35, 35–40]. By adding up to 5 % kaolin, fine dust emission reductions of more than 50 % could be achieved. The use of raw material mixtures has also proven to be effective in reducing fine dust emissions, whereby the sum of aerosol-forming elements is reduced by the addition of a suitable raw material [34, 41–48]. Similar results could be achieved by screening wood chips prior to use in combustion appliances [49, 50].

### **Slagging in the combustion chamber ash**

The low ash softening temperature of herbaceous fuels often leads to strong slagging during biomass combustion, which is caused by melting and subsequent solidification of the ash. Slagging in the firebed can have a negative influence on the burnout of the fuel and leads to increased carbon monoxide emissions. The ash melting behaviour and the associated slagging tendency depend on the one hand on the current combustion chamber or firebed temperature and on the other hand on the composition of the fuel. Particularly a high share of alkali metals potassium and sodium in combination with high chlorine contents or other species, e.g. sulphates, lead to low ash melting temperatures due to the formation of molten salts and the presence of so-called network formers such as silicon and aluminium [4, 9, 12]. There have often been attempts to correlate the ash melting behavior of a fuel



with its fuel composition [51–54]. This would make it possible to predict the slagging tendency from the fuel composition. Sommersacher et al. proposed the index  $(\text{Si}+\text{P}+\text{K})/(\text{Ca}+\text{Mg})$  to allow a prediction based on an almost linear relationship between the fuel composition and the sintering temperature of the furnace ash [11]. Numerous investigations have shown that the addition of calcium-containing additives (e.g. dolomite, limestone, quicklime) increases the ash softening temperature [14, 37, 44, 52, 55–60]. Due to the presence of alkaline earth metals, higher-melting calcium silicates are formed instead of the low-melting potassium silicates, resulting in higher potassium emissions. The addition of the aluminium silicate kaolin also increases the ash melting temperature [14, 34, 37, 56, 57, 59, 61–63]. However, in this case, potassium is preferentially bound as K-Al silicate. Thus the addition of kaolin not only leads to a reduced tendency to slagging but also contributes to a reduced formation of particulate matter. In addition to the addition of mineral additives, the ash melting behavior can also be improved by the use of fuel mixtures. Examples are the admixture of wood to herbaceous fuels [34, 41, 45–47, 64, 65] and the use of biomass peat mixtures [48, 66]. From a technological point of view, it is possible to cool the firebed to prevent sintering and slagging. Water-cooled grates, air-cooled or water-cooled furnace walls or exhaust gas recirculation limit the rise in temperature in the firebed and counteract slagging.

### Deposit formation

For deposit formation, volatile potassium compounds such as KCl,  $\text{K}_2\text{SO}_4$  and  $\text{K}_2\text{CO}_3$  are formed, which are discharged as an aerosol with the exhaust gas stream and which can deposit on heat exchanger surfaces due to their relatively low melting temperatures of about 700–800 °C [2, 67, 68]. On the one hand, these deposits lead to poor heat transfer rates and thus to a reduction in the efficiency of the system. On the other hand, a number of heterogeneous reactions take place on the metal surface with the participation of the compounds contained in the deposit, which strongly contribute to the corrosion of the metal surface. Alkali chlorides play an important role in these so-called high-temperature chlorine corrosion processes. In order to avoid deposits, the use of additives in particular was intensively investigated. Two different approaches are pursued. On the one hand, additives that incorporate KCl can be used. Aluminium silicate-based additives can be used for this purpose. The most important representative of this class is kaolin, which has been successfully used in the incineration of agricultural residues, in particular straw [69]. Other aluminium silicate additives such as zeolite, betonite and emathlite were also investigated. Successful experiments have also been carried out with sewage sludge, which also contains considerable amounts of aluminium silicates, to reduce deposition and the resulting high-temperature chlorine corrosion during the combustion of biomasses with a critical composition [70–72]. As an alternative to aluminium silicate-based additives, sulphur-based additives can also be used. Their effect in preventing high-temperature chlorine corrosion is based on the sulphation of KCl. KCl is converted into  $\text{K}_2\text{SO}_4$ , which is less critical for the formation of deposits due to the higher melting temperature of around 840 °C [73–75]. In addition, the chlorine is released during sulphation as gaseous chlorine gas or hydrogen chloride and discharged with the exhaust gas stream. Thus the sulphation of KCl also contributes to the reduction of high-temperature chlorine corrosion [73, 75].

### Conclusions

In previous research work, a positive effect on the slagging behavior and particulate matter emissions through the use of mineral additives, such as kaolin ( $\text{Al}_4(\text{OH})_8 \text{Si}_4(\text{O}_{10})$ ) and dolomite ( $\text{CaMg}(\text{CO}_3)_2$ ), lime ( $\text{CaO}$ ), dolomite lime ( $\text{CaO MgO}$ ) or carbonic lime ( $\text{CaCO}_3\text{MgCO}_3$ ), has been recognized, particularly in the combustion of non-woody biomass. On the other hand, current test series on a laboratory and pilot plant scale have shown a positive effect of novel additives such as gypsum, halloysite

$\text{Al}_2\text{Si}_2\text{O}_5(\text{OH})_4$  (which is used in gas filters of biogas plants and in landfill gas production) or sulphur-containing residues from iron smelting (e.g. iron sulphide) on apparent problems in the combustion of residual wood and other fuels [60, 61, 76–80]. In particular, the way in which the additives are applied (e.g. grain size, place of addition) seems to play a decisive role in the effect on ash-induced combustion problems. For these reasons, further experimental and theoretical investigations are planned for these novel additives within the framework of the REFAWOOD project.

### 3 Cooperation with other bodies

Within the framework of the Era-Net project, there were two levels of cooperation with other bodies. On the one hand, cooperation between the various national funding projects within the framework of the Era-Net was fostered. For the DBFZ and Endress, this included organizational coordination during the course of the project (planning of project meetings, telephone conferences and workshops, etc.) as well as close methodological and content-related coordination (in particular with regard to additive dosing, analytics, performance of combustion tests, exchange of legal framework conditions and input to LCA analyses).

On the other hand, the project partners DBFZ and Endress had to cooperate with other external bodies as part of their national funding project. The DBFZ was in close contact with the University of Leipzig to perform the XRD analyses. In addition, an intensive exchange was maintained with Gericke in order to meet the challenges of dosing recycled gypsum. The DBFZ contacted Gips Recycling Nederland BV (for the recycled gypsum) and PTH Intermark Poland (for halloysite) to procure the additives. In order to realize the combustion tests on an industrial scale, Endress worked very closely with a plant operator from their client pool in order to coordinate the necessary time and organizational changes in the operating procedure (modification of the measuring section, access to the site, delivery and use of the fuels, intervention in plant operation, etc.). Furthermore, Endress worked closely with fuel suppliers (Speedmaster GmbH in Steinsfeld and Lechner in Wolframs-Eschenbach) to sample and procure the fuels for the trials in WP1 and WP3.

## II. Results

The Era-Net project was divided into a total of 6 work packages (WP). The project is displayed schematically in Figure 1. The main work of the German Era-Net partners was focused on pelleting and combustion tests on bench scale (WP1, DBFZ) as well as the development and testing of an additive dosage into the fuel auger of an industrial heating system (WP3, Endress and DBFZ). In WP1, the fundamental influence of the novel fuel additives on agglomeration, slagging and contamination behavior as well as on emission formation during combustion of residual and used wood was first investigated. The results were then used in WP3 as a basis for examining these concepts on an industrial scale by means of combustion tests in an industrial heating system in order to demonstrate the integration of additives in the fuel supply chain under legal, technical and economic aspects. The case studies were based on the combustion plants and fuel/additive mixtures used in WP3, which were prepared by the partner BE2020+. Based on the results from WP2 and WP3, life cycle analyses were carried out in WP4 (by Utrecht University) for the systematic analysis of the environmental impacts when using the novel fuel additives. As far as possible, site-specific data from the case studies

were used for this purpose. Within the framework of WP5 (responsible Rise, formerly SP), the relevant results of the project were disseminated to specific target groups using suitable instruments.

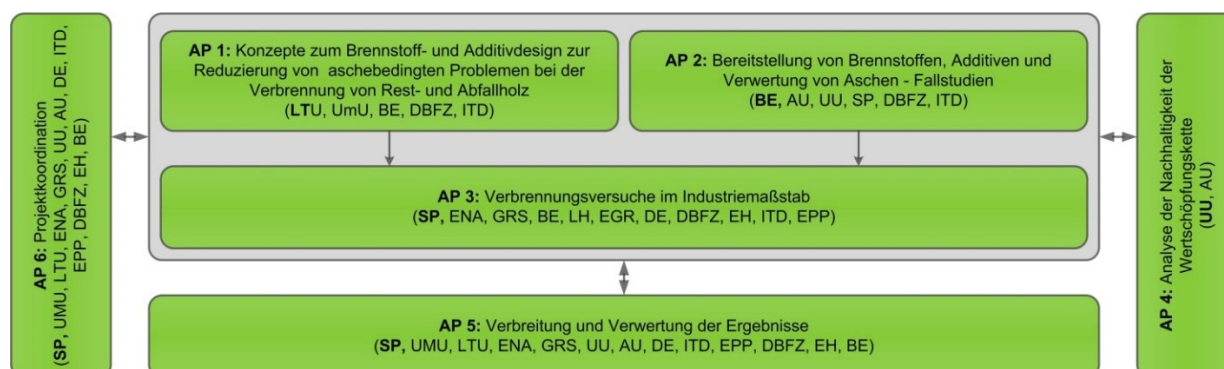


Figure 1: Structural plan (SP: Technical Research Institute of Sweden, UMu: Umeå University, LTU: Luleå University of Technology, ENA: ENA Energy AB, GRS: Gips Recycling AB, UU: Utrecht University, AU: Avans University of Applied Sciences, DE: Dekra, ITD: Instytut Technologii Drewna, EPP: EcoPowerPlant Sp. z o.o., DBFZ: Deutsches Biomasseforschungszentrum gemeinnützige GmbH, EH: Endress Heizanlagen GmbH, BE: Bioenergy 2020+ GmbH)

## 1 Materials and methods

### 1.1 Raw material procurement and fuel production

Forest residual wood chips (1.5 t) and residues from chipboard processing (3 t) were procured as raw materials, with the latter being characterized by a high proportion of fines (> 60%), which made material handling more difficult, Figure 2. Gypsum (G) and halloysite (H) were used as additives



Figure 2: Photos of the raw materials procured within the framework of the project (left: forest residues, right: residues from chipboard processing)

The additives for all tests in WP1 and WP3 were procured in sufficient quantities and delivered to the DBFZ (approx. 4 t each). The results of the analyses are presented in Table 1. The silicon content (G, H) and the very high iron and titanium content (H) showed that both additives were contaminated.

Table 1: Mean values of the fuel and additive analyses (n.a.: not analyzed, n.d.: not detectable; wf: anhydrous)

Parameter	Unit	Wood logging residues (WLR)	Residues from chipboard processing (WCB)	Gypsum (CaSO <sub>4</sub> 2H <sub>2</sub> O)	Halloysite (Al <sub>2</sub> (Si <sub>2</sub> O <sub>7</sub> ) 2H <sub>2</sub> O)
Number of samples	-	5	10	1	1
Water content	wt.-%	8,62	5,53	9,04	2,73
Ash content	wt.-% d.b.	2,99	1,59	n.a.	n.a.
N	wt.-% d.b.	0,73	3,86	n.a.	n.a.
S	wt.-% d.b.	0,05	0,03	17	0,05
Cl	wt.-% d.b.	0,04	0,03	n.a.	0,01
Al	mg/kg d.b.	747	349	2390	157000
Pb	mg/kg d.b.	8,84	6,38	n.d.	1600
Ca	mg/kg d.b.	6960	2090	245000	4850
Fe	mg/kg d.b.	319	179	1580	164000
K	mg/kg d.b.	2680	718	1030	n.d.
Mg	mg/kg d.b.	808	330	3060	2370
Na	mg/kg d.b.	78	205	369	354
P	mg/kg d.b.	550	115	144	3040
Si	mg/kg d.b.	5570	864	14000	155000
Ti	mg/kg d.b.	42	1800	992	23600

The wood logging residues had a particle size class of G30 and a bulk density of 231 kg/m<sup>3</sup>. The residues from chipboard processing are characterized by a bulk density of 337 kg/m<sup>3</sup> and >60 wt.% of the fuel mass have a particle size < 3.15 mm. The bulk density of gypsum and halloysite is 703 kg/m<sup>3</sup> and 1080 kg/m<sup>3</sup> respectively. To ensure a stable combustion process in the 30 kW combustion appliance, the residues from chipboard processing must be pelletized together with the additives due to the high fines content. In order to ensure the best possible comparability of the combustion tests, wood logging residues were also pelletized.

The required admixing quantity of the additives (for WP1 and WP3) was determined on the basis of the analyses and thermodynamic equilibrium calculations listed in Table 1 using the Factsage software (by the WP leader Umea University). Equations were derived from the calculations in order to determine the required admixture quantity of the additives individually for the fuels to be used:

- $S_{add} = (F_{stoich} ((K+Na)/2 + Zn + Pb) - 0,64 S_{fuel}) / 0,64$  for gypsum in mol/kg d.b.
- $Alk_{cap} = Al_{add} - (K_{add} + Na_{add} + 2(Ca_{add} + Mg_{add}))$  with  $Amount_{add} = (K_{fuel} + Na_{fuel}) / Alk_{cap}$  for halloysite in mol/kg d.b.

This resulted in the following additive admixtures, whereby a stoichiometric factor (F) of 1.5 was selected for the additive admixture:

- Wood logging residues, WLR:
  - gypsum: 13.4 kg additive / t dry fuel
  - halloysite: 31.7 kg additive / t dry fuel
- Residues from chipboard processing, WCB:
  - gypsum: 4.3 kg additive / t dry fuel
  - halloysite: 10.6 kg additive / t dry fuel

However, to ensure the quality of the test results (contrary to the planning) a complex homogenization of the raw materials was necessary. In addition, the wood logging residues and chipboard materials had to be screened beforehand in order to remove any impurities and avoid damage to the pellet press, Figure 3. Also, a very high dust generation during comminution and increased wear on the hammers during comminution of the raw materials in the hammer mill had to be observed, Figure 3. Furthermore, only limited results are available in the literature and experience for the pelleting of these raw materials, since they are typically used unpelletized in larger plants. However, pelletizing with corresponding preliminary tests is indispensable for trials on a pilot plant scale. Accordingly, there were delays in the production of the additive pellet batches for the trials in the pilot plant.

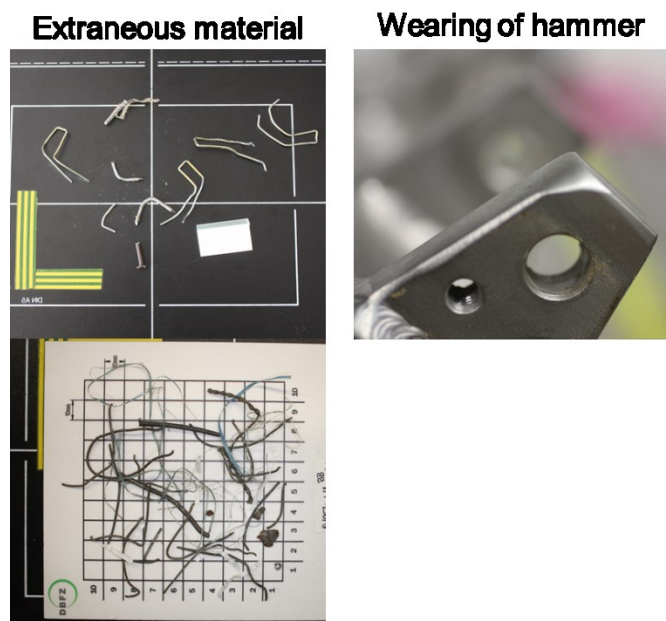


Figure 3: Impurities in the fuels (left) and abrasion of the hammer of the mill (right)

Since the residues from chipboard processing had a share of fines, fractionation by sieving was carried out in order to reduce the process step of comminution. A sieve mesh width of 3 mm was used. The sieve passage (>3 mm) amounted to approx. 55 wt.%. In order to generate a pelletizable material, the remaining 45 % by weight was crushed using a hammer mill (type CHP 230/200-N3 from Netzsch) and a sieve insert with a sieve hole width of 4 mm. This grain size reduction is also achieved with the WLR.



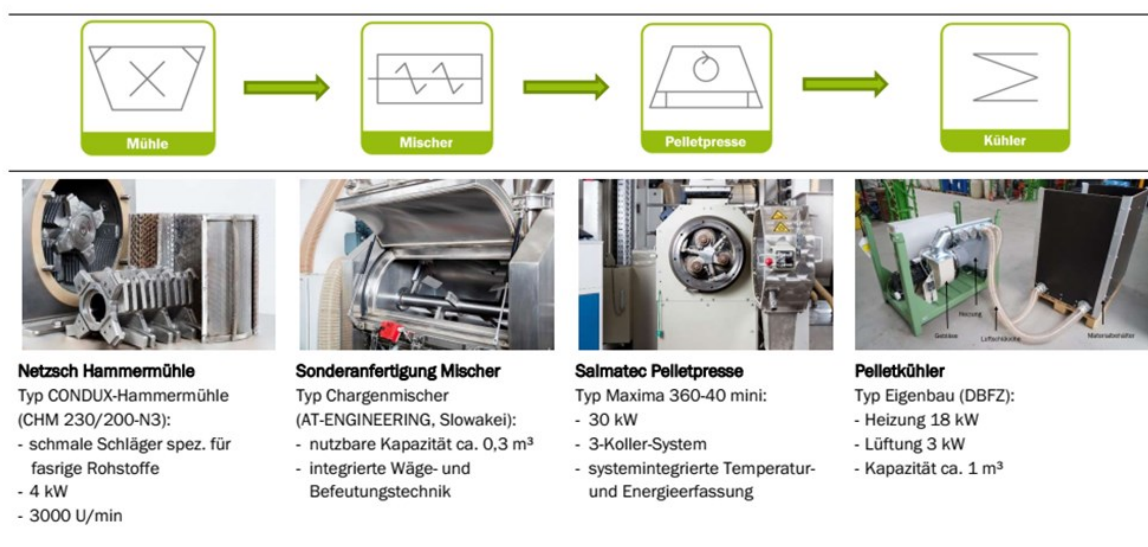


Figure 4: Pelletizing at the DBFZ divided into the relevant process steps and the corresponding devices

The pelleting tests followed the process shown in Figure 4, starting with comminution, conditioning (mixing and adjusting the water content), compacting and final cooling. The relevant technical process settings such as water content of the material, press channel length of the die, distance between the roller and die and speed of the die or feed screw are listed in Table 2. Mechanical durability ( $\geq 97.5$  wt.%) and bulk density ( $\geq 600$  kg/m<sup>3</sup>) shall be in accordance with DIN EN ISO 17225-2. In parallel, the specific energy consumption of the pelleting process is determined.

Table 2: Process parameters for pellet production of the fuel pellet batches

Parameter	WLR-Pellets	WCB-Pellets
Conditioning Water content	20 ± 0.5 wt.-%	22.5 ± 0.5 wt.-%
Die geometry (ØxL)	6x30 mm	6x30 mm
Distance die - roller	0,25 mm	0,25 mm
Die power	100 %	100 %
Screw performance	45 %	45 -50 %
Shear blade distance	30 mm	30 mm

A paddle mixer with a volume of 0.3 m<sup>3</sup> was available for conditioning to a certain water content. Accordingly, 30 kg per batch could always be conditioned for WLR and WCB. The subsequent pelleting is carried out with a SALMATEC ring die press including a three-roller system (type Maxima 360-40 mini) with a capacity of 30 kW. During compaction, specific energy consumption, throughput and process temperatures were recorded.

In order to identify relevant process parameters such as water content of the material, length of the press channel of the die, distance between the roller and the die and speed of the die or feed screw, preliminary tests were carried out. Besides the general feasibility, the pellets made of WLR and WCB should have comparable physical-mechanical properties.

## 1.2 Combustion tests on bench scale

The combustion tests were carried out with the fuels described in Chapter 1.1, Table 3. In addition, combustion tests with the reference fuel ENplus wood pellets (Class A1) were carried out for comparison purposes

Table 3: Test matrix for the combustion tests on a small combustion plant in the pilot plant of the DBFZ

Abbreviation	Description	Fuel	Load	Emissions	Analysis of combustion chamber ash	Analysis of fine dust
WLR	Wood logging residues without additive	Pellets	Full load	O <sub>2</sub> , CO, NO <sub>x</sub> , SO <sub>2</sub> , HCl, H <sub>2</sub> O, total particulate matter	Chemical composition, XRD, classification (see Chapter 1.4)	Chemical composition (see Chapter 1.4), XRD
WLR+G	Wood logging residues with 13.4 kg gypsum / t dry fuel	Pellets	Full load			
WLR+H	Wood logging residues with 31.7 kg halloysite / t dry fuel	Pellets	Full load			
WCB	Residues from chipboard processing without additives	Pellets	Full load			
WCB+G	Residues from chipboard processing with 4.3 kg gypsum / t dry fuel	Pellets	Full load			
WCB+H	Residues from chipboard processing with 10.6 kg halloysite / t dry fuel	Pellets	Full load			
Clean wood	Wood pellets (ENplus, class A1)	Pellets	Full load			

The employed boiler is designed for the combustion of wood pellets (ENplus, DINplus), wood chips (P16B or P45A (very good quality) according to ISO17225-4 [81], water content <30 wt.-%) as well as cereal grains and has a nominal heat output of 30 kW (if wood pellets are used). The system has a moving step grate and a staged combustion air supply. The primary air is supplied to the combustion chamber via the grate. The secondary air is supplied tangentially to the combustion gas in the burnout zone in order to achieve good mixing and optimum gas burnout in the secondary zone. The fuel is automatically ignited by means of a hot air blower. A moving step grate ensures automatic grate cleaning, movement in the firebed and ash removal during combustion. The system is equipped with an electronic combustion control by means of a lambda sensor. The hot combustion gases are directed into the chimney with the aid of an induced draft via a self-cleaning shell-and-tube heat exchanger.

For the combustion tests, the furnace was integrated into a heating network in order to enable continuous plant operation. The combustion tests were carried out at full load under conditions as stationary as possible. On the flue gas side, the boiler was connected to a suitable measuring section in order to record all relevant emission measured variables and plant parameters. The flue gas measuring section met the requirements of EN 13284-1:2002 [82]. The chimney draught was set to 15 Pa.

For each combustion test, the boiler was operated at full load and adapted to the specific requirements of the fuels used, with the aim of ensuring (i) low CO and NO<sub>x</sub> emissions, (ii) minimized slag formation in the bottom ash and (iii) sufficient ash removal. To meet these requirements, adjustments to the primary and secondary combustion air supply, the set point for the oxygen in the flue gas and the grate operation were required. The boiler operating parameters optimized for each fuel were used for the full load combustion tests without further adjustments. In each combustion test the O<sub>2</sub>, CO, NO<sub>x</sub>, SO<sub>2</sub> and HCl emissions were recorded continuously with an FTIR, type CX-4000 (ANSYCO GmbH) and an O<sub>2</sub> analyzer, type PMA 100-L (M&C TechGroup Germany GmbH). The sampling line and the probe were heated to 180 °C. With stable boiler operation, emission values were recorded over a period of approx. 5 hours. Subsequently, 30 min mean values were calculated, which were used for the calculation of the total mean value.

In parallel, the total particulate matter emission (TPM) in the flue gas was measured according to the gravimetric method according to VDI 2066 [83], whereby the out-stack method and the automatic isokinetic control unit ITES (Paul Gothe GmbH) were used for sampling. The sampling probe had a diameter of 6 mm and was heated to 160 °C to avoid condensation of flue gas components. The sampling time was at least 30 minutes for each measurement and was performed at least three times for each combustion experiment. A plane filter (Munktell MK360 with retention > 99.998 %, diameter 45 mm) was used to collect the particles. Before the measurement, the plane filter was pretreated by drying at 180 °C for at least 1 h and then cooled down to ambient temperature and conditioned in a weighing chamber with constant temperature and humidity for at least 8 h. The plane filter was then dried at 180 °C for at least 1 hour. After the measurement, the plane filter was dried for at least 1 h at 160 °C and additionally cooled down to ambient temperature and conditioned in a weighing chamber with constant temperature and humidity for 8 h. The filter was then dried for at least 1 h at 160 °C. The filter was then dried for at least 2 hours in a weighing chamber with constant temperature and humidity. After each combustion test, the sampling probe was cleaned with distilled water and acetone (HPLC quality) and then dried with oil-free compressed air. The flushing liquid obtained was analyzed according to VDI 2066 for the residual mass of the particles, which were evenly distributed over each TPM measurement of the combustion test. In addition, the particles in the flue gas were collected in parallel using the same heated sample probe, a PTFE filter and a vacuum pump instead of the Munktell filter. After the measurement, the collected ash was removed from the PTFE filter and further analyzed.

After the boiler was completely cooled down, the bottom ash from the ash box and from the grate were collected, combined and weighed for further analyses and classifications. Finally, the primary and secondary combustion chambers as well as the heat exchanger were thoroughly cleaned with an industrial vacuum cleaner.

### 1.3 Industrial-scale combustion tests

The combustion tests on industrial scale were carried out in an Endress combustion plant (nominal heat output 800 kW, type USF-W, year of construction 2014), Figure 5 and Figure 6. All necessary preparations for the field measurements were mainly organized by Endress in cooperation with the DBFZ and the plant operator (e.g. for installation of additional measuring points in the flue gas path, fuel procurement and delivery, installation of the dosing unit, assessment of the previous plant



operation). The tests took place in March 2018 (with WLR) and January 2019 (with WCB). The DBFZ supported Endress in the measurement of emissions as well as fuel and ash sampling.

The furnace is equipped with a 4-sided ventilated underfeed combustion chamber, an automatic ash discharge and a temperature-controlled ignition fan and has a fully automatic power and combustion control. The resulting exhaust gases are discharged via an automatically cleaned heat exchanger, where the exhaust gases in front of the chimney are cleaned of coarse particles by means of a multi-cyclone.

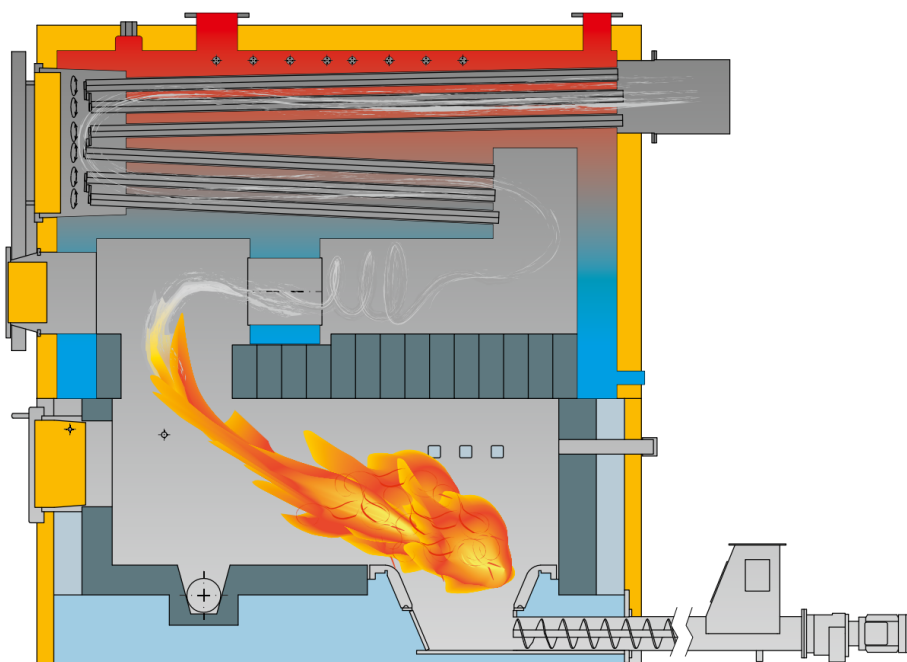


Figure 5: Schematic of the Endress combustion plant, type USF-W 800

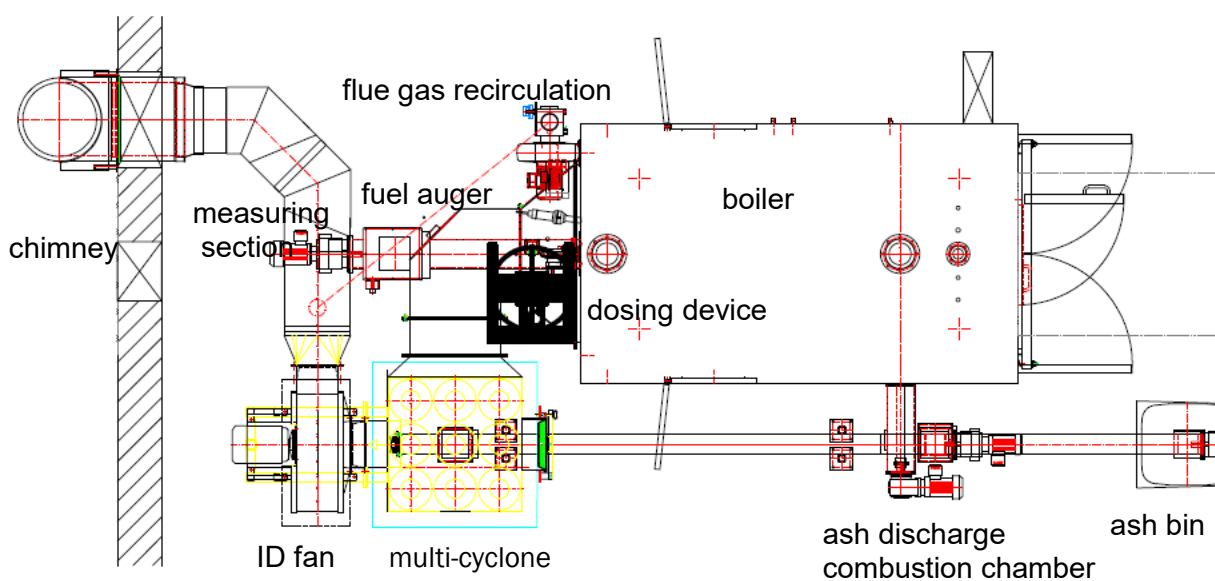


Figure 6: Installation plan of the Endress combustion plant, type USF-W 800 incl. additive dosing unit (top view)

For technical reasons, Endress combustion plants only allow the additives to be added into the fuel auger before the fuel is introduced into the combustion chamber. However, the dosing technology offered by Endress is clearly too large for the required additive throughputs (between 0.5 and 7 kg/h). Accordingly, GERICKE laboratory dosing technology (type GLD87) available at the DBFZ was tested and the conveying characteristics for gypsum and halloysite at different conveying rates (frequency converter (FU) at 5%, 50% and 100%) were determined. In consultation with the plant operator, the mechanical and electrical integration of the additive metering system into the stoker screw of the industrial furnace was then carried out by Endress, Figure 6. The quantity of additive to be used is described in Section 1.1.

Furthermore, the existing measuring section (Figure 7) had to be modified for the emission measurements in order to acquire the required emission parameters. This was mainly carried out by Endress in coordination with the DBFZ. The measuring section is located after the chimney fan and has a round cross-section with a straight length of 2.1 m, Figure 7.

Due to the mild weather conditions and due to the low connection rate of the local heating network, only a small amount of heat could be released to the 20,000 litre buffer storage tank. Thus, only 1-1.5 full load hours were available per test day. Figure 8 shows a typical plant operation based on various plant temperatures and the O<sub>2</sub> content in the exhaust gas. Table 4 shows the test and analysis matrix for the field measurements.

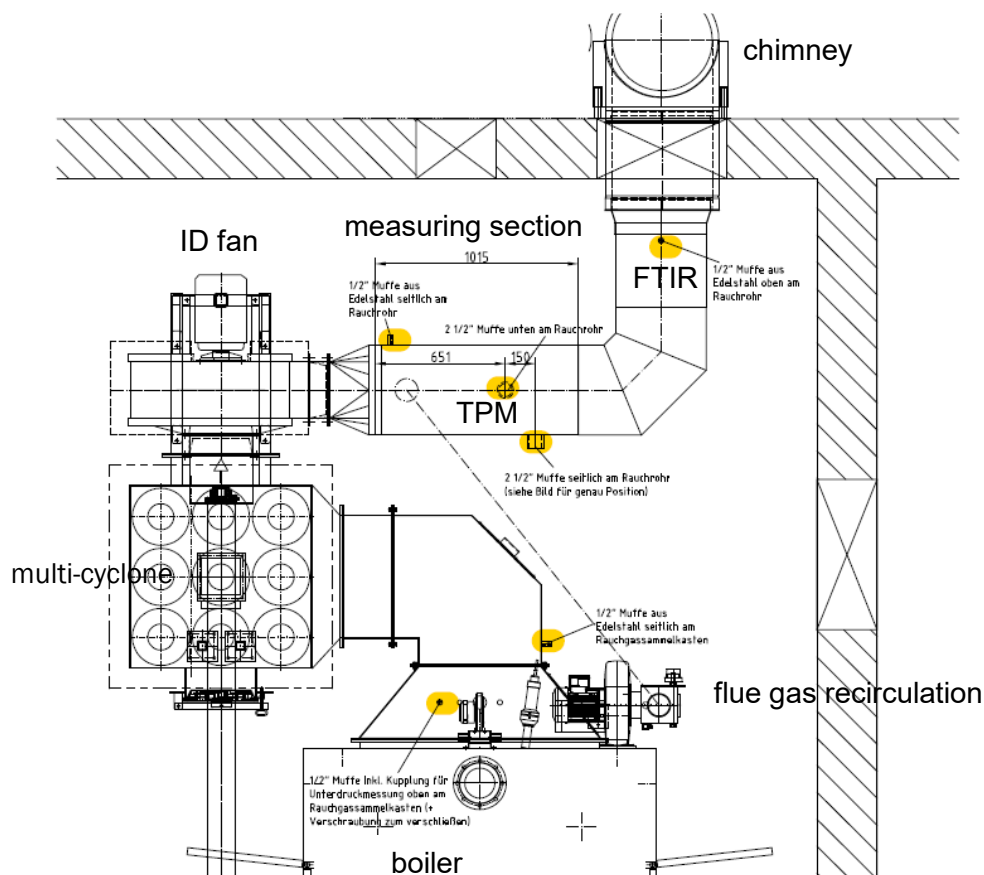


Figure 7: Installed measuring section at the Endress combustion plant, type USF-W 800 (plan view)

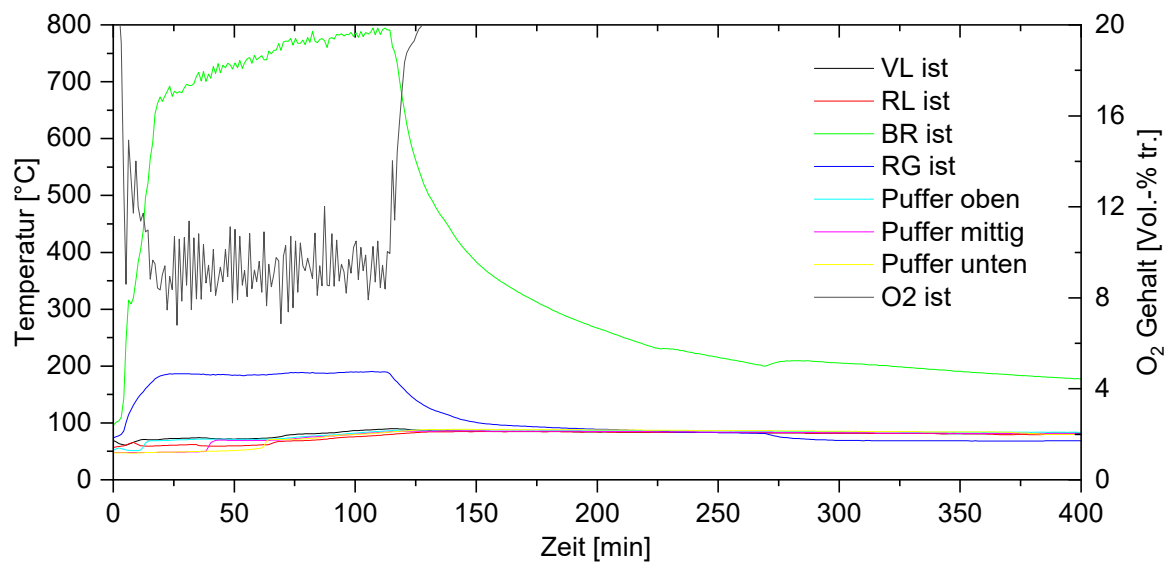


Figure 8: Typical temperature curve at certain points in the heating circuit of the 800 kW furnace for WLR+G (VL: hot water inlet temperature, RL: hot water return temperature, BR: combustion chamber temperature, RG: flue gas temperature).

Table 4: Test matrix for the combustion tests at the Endress combustion plant, type USF-W 800

Abbreviation	Description	Fuel	Load	Emissions	Analysis of combustion chamber ash	Analysis cyclone ash	Analysis fine dust
WLR	Wood logging residues	Wood chips	Full load			-	-
WLR+G	Wood logging residues with 13.4 kg gypsum / t dry fuel	Wood chips	Full load			-	-
WLR+H	Wood logging residues with 31,7 kg halloysite / t dry fuel	Wood chips	Full load	O <sub>2</sub> , CO, NO <sub>x</sub> , SO <sub>2</sub> , HCl, H <sub>2</sub> O, total particulate matter	Chemical composition, XRD, classification (see Chapter 1.4)	-	-
WCB	Residues from chipboard processing without additive	Sawdust	Full load			Chemical composition, XRD, classification (see Chapter 1.4)	Chemical composition, XRD, classification (see Chapter 1.4)
WCB+G	Residues from chipboard processing with 4.3 kg gypsum / t dry fuel	Sawdust	Full load				
WCB+H	Residues from chipboard processing with 10.6 kg halloysite / t dry fuel	Sawdust	Full load				

The following samples were taken during the industrial scale combustion tests:

- Gaseous emissions (continuous): O<sub>2</sub>, H<sub>2</sub>O, CO, NO, NO<sub>2</sub>, HCl, SO<sub>2</sub>, CH<sub>4</sub>, N<sub>2</sub>O, NH<sub>3</sub> by means of a mobile FTIR developed at DBFZ.
- Total particulate matter (discontinuously according to VDI2066-1 [83] (out-stack method, sampling probe with a diameter of 6 mm, sampling time was at least 15 min for each measurement and was repeated at least two times for each combustion experiment), see chapter 1.2. For organizational reasons, the total dust measurements were carried out with WLR, WLR+G and WLR+H with a Wöhler SM 500 during combustion.
- At least 3x PTFE filters to measure the composition of the total particulate matter (max. 1 hour per measurement), see Chapter 1.2 and 1.4.
- Sampling of fuel: Every test day, about 1 kg of fuel per hour was taken manually between the discharge screw and the fuel auger. The samples were summarized and analyzed for WLR and WCB.
- The complete bottom ash was obtained for each experiment and analyzed using the methods described in Chapter 1.4. For this purpose, the bottom ash remained in the combustion chamber and the ash discharge screw was collected on the following day and then the combustion chamber was completely cleaned so that the next combustion test could take place.
- The cyclone ash was taken continuously between the beginning of the first and the end of the last PM sampling. For this purpose, a separate ash container was positioned in the ash discharge of the multicyclone during the measuring time. The samples were then analyzed using the methods described in Chapter 1.4.
- In each experiment, the additive quantity consumed was determined by weighing the additive quantity before and after the experiment using a balance (measuring range up to 6 kg, reading accuracy 0.01 kg). The dosing tools and the delivery rate were calculated and adjusted according to the determined characteristic data and the expected fuel consumption.
- The analysis of the flue gas-side deposits or corrosion processes on the heat exchanger during combustion is difficult to implement for small and medium-sized combustion plants for heat supply due to their design. Available sampling devices have so far only been used in power plants. In addition, only a very short test duration could be realized for each experiment, which meant that representative sampling was not possible. Therefore, sampling to determine flue gas-side deposits and corrosion processes during the combustion tests in WP3 was not performed.

## 1.4 Fuel and ash analysis

Fuel analysis, sampling and sample preparation were carried out in accordance with European standards for solid biofuels [84-86]. The following parameters were analyzed: Water content, ash content (550 °C), total sulphur and chlorine, main elements (i.e. Al, Ca, Mg, P, K, Si, Fe, Ti, Mn and Na, hydrofluoric digestion, ICP-OES) and secondary elements (i.e. Cd, Cr, Cu, Pb and Zn, hydrofluoric digestion, ICP-OES).

In addition, the entire bottom ash was collected after the combustion tests in WP1 and analyzed in order to estimate the sintering degree in the slag according to the respective fuel. The completely

recovered ash samples from the combustion tests were sieved using a set of round hole sieves (<63 mm, <45 mm and <16 mm) according to a method previously developed by Öhman et al. [87] and the proportion of each sinter fraction was quantified as a percentage by weight and evaluated with regard to its degree of sintering. Furthermore, the complete ash samples taken during the combustion tests in WP1 and WP3 were ground and homogenized for the analysis of main and secondary elements according to the European standards for solid biofuels and analyzed as described above. Chlorine was determined in the eluate according to DIN EN 12457-4 [88].

The ash (WP1 and WP3) recovered from the PTFE filter and the cyclone ash (WP3) were recovered and analyzed for main and secondary elements as described above.

For the XRD analysis, the ash samples were grinded and transfed to a glass sample carrier and analyzed in an X-ray diffractometer of the type BRUKER D8 DISCOVER with a 2D surface detector of the type VANTEC-500 (sample distance 30 cm). The X-ray source generates CuK $\alpha$  radiation (1.5418 Å), while the anode operates at a current strength of 40 mA and a voltage of 40 kV. The X-ray beam is adapted with a snout (pinhole) of 1.0 mm diameter and a microcollimator of 0.5 mm diameter. Scanning was performed at a scattering angle of 5 to 85 ° (step width=0.005°, sampling rate=2s/step). During the measurements, the samples were rotated azimuthally at 72° per minute. The analysis of the diffractograms was done with the software Match! and the Crystallography Open Database (version REV211633 2018.10.25). The existing phases and their proportions were determined using the semi-quantitative "Reference Intensity Ratio" (RIR) method.

## 2 Achieved results

### 2.1 Fuel production

During the pelleting of WCB, the adhesive present in the WCB reacts with water and temperature. Apparently, the material in the press channel hardens, so that the pellets can no longer be pushed out of the die. Thus the pellet mill got stuck. As a result, the material had to be removed by manually from the die. With higher initial water content, a continuous operation of the pellet mill was possible.

Table 5: Results from the production of fuel pellets (WLR: forest residues, WCB: residues from chipboard processing, G: gypsum, H: halloysite)

DBFZ-batch number	Material	Pellet mass	Bulk density	Mechanical durability	Production-related fines	Pellet throughput	Specific energy consumption
		kg	kg/m <sup>3</sup>	wt.%	wt.%	kg/h	kWh/kg
TK - 01854-056	WLR	88.1	645	92.9	25.9	70.5	0.30
TK - 01854-063	WLR+G	62.2	674	94.6	15.8	79.4	0.27
TK - 01854-064	WLR+H	74.4	648	93.9	11.7	127.5	0.19
TK - 01853-069	WCB	113.4	525	93.3	16.4	104.7	0.20
TK - 01853-070	WCB+G	89.4	614	96.1	11.3	90.9	0.22
TK - 01853-071	WCB+H	89.1	600	95.2	15.1	87.9	0.17



Table 5 shows the results of the main tests. It is shown that all pellet batches, with the exception of the WCB batch, comply with the limit value for pellet bulk density from DIN EN ISO 17225-2 ( $\geq 600 \text{ kg/m}^3$ ). However, the determined mechanical durability of all fuel batches is clearly below the specifications of the fuel standard (i.e.  $< 97.5 \text{ wt.}\%$ ). There is a need for further research with regard to the optimal experimental parameters. The compression of WLR basically had a higher specific energy requirement than the pelleting of WCB. A possible reason can be found in the higher ash contents in connection with increased friction forces in the press channel. However, it should be noted that the WCB was pelleted with higher water contents ( $22.5 \pm 0.5 \text{ wt.}\%$ ), with water reducing the frictional forces in the die. Interestingly, the addition of halloysite reduces the specific energy requirement of the pelleting process, both for WLR and WCB.

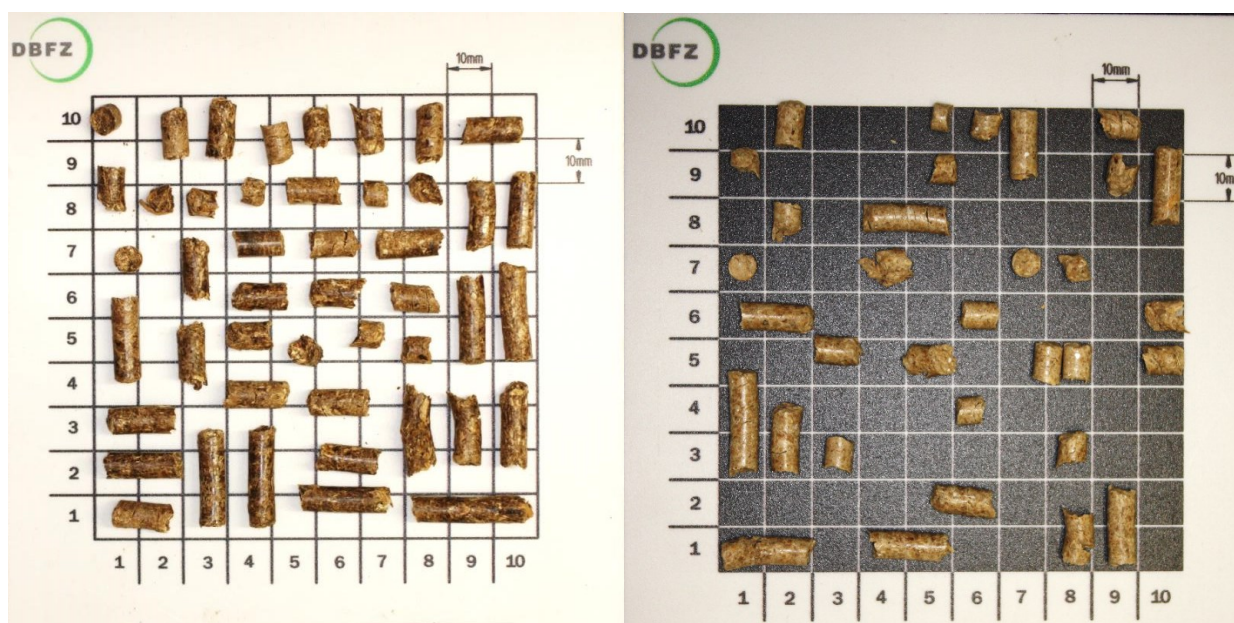


Figure 9: Fuel pellets from WLR without additive (left) and WCB without additive (right)

The pellets produced are shown as examples in Figure 9. The produced fuel pellets are characterized by an overall good mixing quality between the raw materials and the additives, Table 6. The comparison of the analyzed values with calculated values from the pure components (WLR, WCB, G and H) showed only some differences:

- WLR+G had a value more than 20% lower for S and more than 20% higher for Si.
- WLR+H was more than 20 % higher for Si.
- WCB+G had more than 20 % lower values for K

The fuel analysis also showed that the N and Ti content of WCB was at least eight times higher compared to WLR, Table 6. The addition of both additives increased the ash content in the fuels to up to 6.15 wt.% d.b. (for WLR+H). The addition of gypsum led to Ca and S contents 3-4 times higher than those of pure fuels. In contrast, Al, Fe and Si were significantly increased by using halloysite as an additive. This also applies to Ti in WLR. The content of K, Mg, Cl remained largely unchanged. This trend is also reflected in the fuel indices. Thus,  $\text{Si}/(\text{Ca}+\text{Mg})$ ,  $(\text{Si}+\text{P}+\text{K})/(\text{Ca}+\text{Mg})$ ,  $\text{Si}/\text{K}$  were highest for fuels added with halloysite, indicating a higher risk of slag formation in the furnace. The addition of gypsum mainly affected the 2S/Cl ratio.

Table 6: Analysis of additives and fuel pellets used WLR: wood logging residues, WCB: residues from chipboard processing, G: gypsum, H: halloysite)

Parameter	Unit	WLR	WLR+G	WLR+H	WCB	WCB+G	WCB+H	Clean wood
Bulk density	kg/m <sup>3</sup>	661	671	648	569	614	600	633
Mechanical durability	wt.-%	95.69	94.2	93.9	94.3	96.1	95.2	99.0
Water content	wt.-%	8.58	9.43	9.03	11.1	10.40	11.70	9.0
Lower calorific value, H <sub>u</sub>	MJ/kg d.b.	18.54	18.33	17.99	18.48	18.38	18.30	19.3
Ash content, A	wt.-% d.b.	3.10	4.53	6.15	1.49	1.79	2.26	0.33
N	wt.-% d.b.	0.50	0.47	0.45	4.33	4.37	4.15	0.21
Cl	wt.-% d.b.	0.012	0.011	0.012	0.026	0.026	0.028	0.01
S	wt.-% d.b.	0.045	0.200	0.048	0.027	0.093	0.028	0.004
Al	mg/kg d.b.	671	820	5190	505	424	1790	15.5
Pb	mg/kg d.b.	bld	bld	46.3	7.2	6.5	24.0	1.9
Cd	mg/kg d.b.	0.2	0.2	0.5	0.2	0.2	0.3	0.3
Ca	mg/kg d.b.	4650	7140	4950	2450	3370	2360	777
Cr	mg/kg d.b.	9.5	11.4	25.5	5.6	5.5	11.0	0.72
Fe	mg/kg d.b.	298	333	5250	227	233	2030	34
K	mg/kg d.b.	2310	2330	2400	453	390	295	497
Cu	mg/kg d.b.	3.3	3.4	8.6	10.1	10.3	12.6	1.03
Mg	mg/kg d.b.	631	651	712	389	403	392	115
Mn	mg/kg d.b.	290	292	344	83.5	82.7	102	115
Na	mg/kg d.b.	73.3	85.9	92.6	262	237	232	9.2
Ni	mg/kg d.b.	2.8	2.8	13.8	1.4	1.5	5.4	0.28
P	mg/kg d.b.	446	461	540	137	130	154	55.5
Si	mg/kg d.b.	5200	6720	12500	937	866	2140	137
Ti	mg/kg d.b.	26.0	45.5	546	2400	2070	2280	3
Zn	mg/kg d.b.	27.3	26.9	42.9	39.5	38.2	43.7	10.9
(K+Na)/(2S+Cl)	mol/mol	1.98	0.50	1.96	0.95	0.31	0.70	2.3
Si/(Ca+Mg)	mol/mol	1.30	1.17	2.91	0.43	0.31	1.02	0.20
(Si+P+K)/(Ca+Mg)	mol/mol	1.82	1.53	3.43	0.64	0.45	1.18	0.8
Si/K	mol/mol	3.13	4.01	7.25	2.88	309	10.1	0.38
2S/Cl	mol/mol	8.29	40.2	8.85	2.30	7.91	2.21	0.80



## 2.2 Combustion tests on a pilot plant scale

The boiler could be operated satisfactorily with an excess air between 1.6 and 2.0. Thus the average CO emissions from the combustion of all fuels were at a low level ( $< 100 \text{ mg/m}^3$ ), Figure 10. Fluctuations in CO emissions result mainly from the frequent operation of the moving grate and partly also from sintering in the bottom ash. Average  $\text{NO}_x$  emissions range from  $100 \text{ mg/m}^3$  for ENplus wood pellets (Clean Wood) to  $742 \text{ mg/m}^3$  for the WCB+H batch. The emission values correspond to the findings known from other authors [26, 89-94]. Differences in  $\text{NO}_x$  emissions are mainly due to the nitrogen content of the fuel. However, different (primary and secondary) air conditions and sintering tendencies in the combustion chamber ash may also have influenced the formation of  $\text{NO}_x$  emissions to some extent. The combustion of fuels with a high S content led to higher  $\text{SO}_2$  emissions. The combustion of the WLR batches, for example, was characterized by higher  $\text{SO}_2$  emissions compared with the WCB batches. However, the use of gypsum as an additive led to very high S contents in the fuel and thus to the highest  $\text{SO}_2$  emissions of  $252 \text{ mg/m}^3$  for WLR+G. Although the release and retention of S depends on ash chemistry and actual combustion temperatures in the firebed [11, 49, 60, 95], a linear correlation between S content in the fuel and  $\text{SO}_2$  emissions was observed ( $R^2=0.99$ ). As suggested by Rebbling et al. [60], elevated  $\text{SO}_2$  values resulting from the degradation of  $\text{CaSO}_4$  are likely. HCl emissions are at a low level of max.  $15.7 \text{ mg/m}^3$ . In this context, the HCl emissions of WLR are lower than those of WCB combustion. The use of halloysite as an additive led to slightly higher HCl emissions during combustion in both WLR and WCB. This is confirmed by previous test results with kaolin, which has a similar material composition and effect to halloysite [30, 32, 34, 96]. The average total particulate matter emissions (TPM) were between 26 and  $160 \text{ mg/m}^3$ . The highest TPM emissions were found during the combustion of WLR+G. The use of halloysite reduced TPM emissions due to the retention of potassium in the bottom ash [30, 32-34, 63, 79, 97].

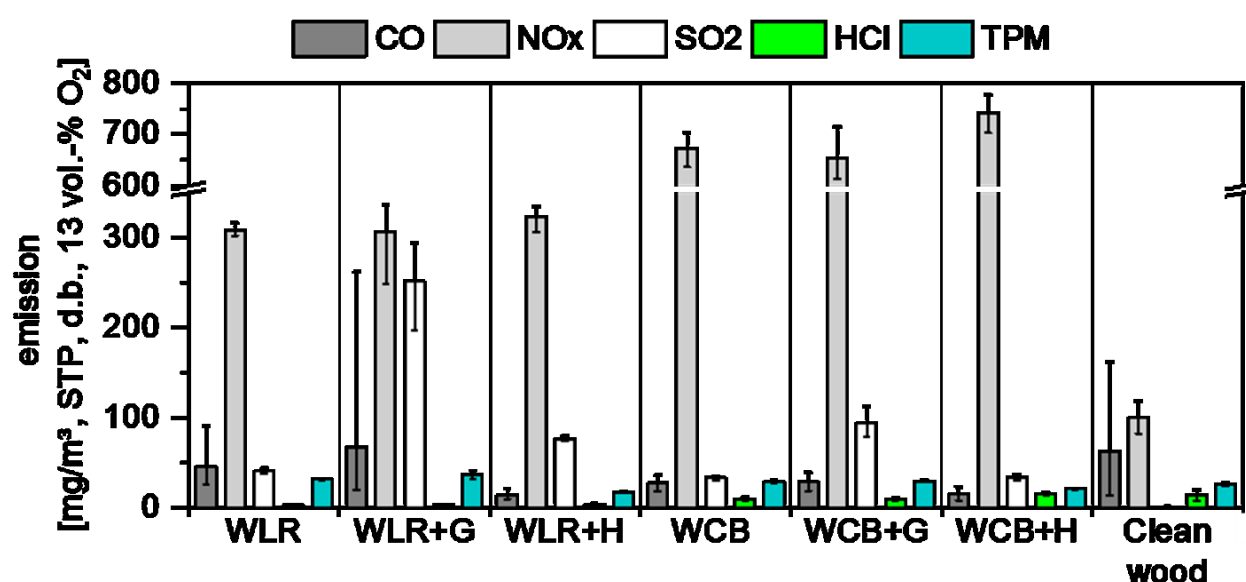


Figure 10: Emissions from the combustion of WLR and WCB pellets with additives (WLR: forest residues, WCB: residues from chipboard production, G: gypsum, H: halloysite, clean wood: ENplus wood pellets / class A1)

Based on the fuel indices, an increased slagging risk in the bottom ash was expected for the combustion of WLR pellets. The classification of the bottom ash according to the method proposed by Öhman et al. [87] resulted in two sintering degrees: i) category 1 (slag-free) for clean wood, WCB and WCB+G and ii) category 2 (partially sintered ash, i.e. particles with clearly melted ash) for WLR, WLR+G, WLR+H, WLR+H, Figure 11.

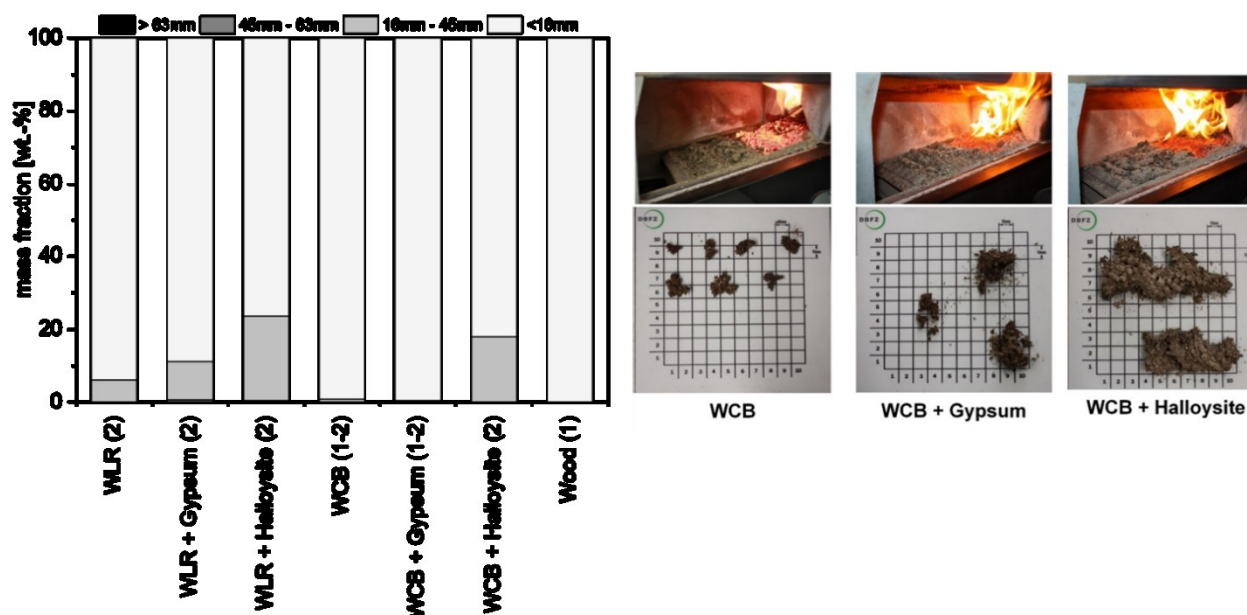


Figure 11: Evaluation of the degree of slagging of the bottom ashes from the combustion of WLR and WCB pellets with additives according to Öhman et al. [87]. (WLR: wood logging residues, WCB: residues from chipboard processing, Wood: ENplus wood pellets / class A1).

For category 1, the share of slag (i.e. agglomerates > 16 mm) in the bottom ash is 0 wt.%, while for the other bottom ashes having category 2, the share of slag may be > 20 wt.%. However, agglomerates > 45mm were not found in the bottom ash. The positive influence of CaO on ash behavior from the decomposition of CaSO<sub>4</sub> proposed by Rebbling et al. [60] cannot be confirmed for the combustion of WLR. In all cases, the use of halloysite produced the highest share of ash agglomerates in the bottom ash, which was most pronounced in the combustion of WLR, Figure 11.

The ash melting behavior depends mainly on the relative concentrations of the ash-forming elements, the absolute amount of critical compounds and their thermodynamic and kinetic properties [98]. But also their spatial distribution in the biomass fuels strongly influences the final ash melting behavior [12]. In addition, some elements used either inherently or as additives may increase potassium retention, e.g. silicon or sulphur [12, 24, 64, 99, 100]. In the presence of Al in the ash, alkali metals could be incorporated as refractory aluminosilicates [37, 39, 40, 101, 102]. At lower temperatures, more potassium is bound into the bottom ash [25, 103]. In particular, the retained fraction is involved in slag formation in the furnace ash [12, 22, 23, 104, 105]. Due to its high volatility, a considerable part of the potassium contained in the fuel can be released into the gas phase during combustion. During combustion, K release is facilitated by the presence of Cl as KCl, S as K<sub>2</sub>SO<sub>4</sub> or in the form of carbonates as well as KOH [12, 22, 23, 104, 105]. However, the behavior of the inorganic components is not fully understood, especially in an oxygen-poor atmosphere (i.e. during pyrolysis and gasification),

which influences the decomposition of the organic and inorganic fractions and thus the release at a given transformation temperature [21-24, 105-109].

The main components of the bottom ashes from the combustion of the pellet fuels used without additives were Si, K and Ca, Figure 12 (left). However, the relative proportion of these elements to the ash-forming substance can vary greatly. In the bottom ash of the reference fuel (clean wood), calcium was the dominant element followed by potassium and silicon, while in the case of WLR calcium and silicon represent a comparably high share in the bottom ash. In WCB, Ti is the main ash forming element followed by calcium and subordinated by Si and K. The very high proportion of Ti in the furnace ashes of WCB can be attributed to the paints and coatings in the starting material [110]. The use of the additives resulted in an increase in the Ca and S concentration (when gypsum is used) as well as in the Fe and Al concentration (when halloysite is used) in the bottom ash. This is also reflected by the XRD analysis of the bottom ashes, Table 8. The ash from batch WLR consisted mainly of  $\text{SiO}_2$ ,  $\text{Ca}_2\text{Mg}[\text{Si}_2\text{O}_7]$ ,  $\text{K}_2\text{Ca}_2(\text{SO}_4)_3$  (MaP) and  $\text{K}_2\text{Mg}_2[\text{SO}_4]_3$ ,  $\text{CaMg}[\text{CO}_3]_2$  (MiP). In contrast, the crystalline phase of the WCB ash was composed of  $\text{Ca}_2\text{Mg}[\text{Si}_2\text{O}_7]$ ,  $\text{K}_2\text{Mg}_2[\text{SO}_4]_3$ ,  $\text{MgO}$  (MaP) and  $\text{CaCO}_3$ ,  $\text{Ca}_3\text{Mg}(\text{SiO}_4)_2$ ,  $\text{SiO}_2$  (MiP). Thus the bottom ashes of the pure fuels are dominated by relatively high melting phases (especially  $\text{SiO}_2$ ,  $\text{Ca}_2\text{Mg}[\text{Si}_2\text{O}_7]$ ,  $\text{Ca}_3\text{Mg}(\text{SiO}_4)_2$  und  $\text{MgO}$ ). The use of gypsum in WLR led to an increased formation of  $\text{KAlSi}_2\text{O}_6$  and, to a lesser extent, to the formation of lower-melting sulphates ( $\text{K}_2\text{Ca}_2(\text{SO}_4)_3$ ). This may be the reason for the slightly higher proportion of sintering in this bottom ash, Figure 11. The use of gypsum in the combustion of WCB led to the increased formation of relatively high-melting Ca-Al silicates  $\text{Ca}_3\text{Al}_2\text{O}_6$ , whereby less  $\text{Ca}_3\text{Mg}(\text{SiO}_4)_2$ ,  $\text{K}_2\text{Mg}_2[\text{SO}_4]_3$  and  $\text{KAlSi}_2\text{O}_6$  were formed. Thus a negative impact on the sintering behavior during combustion is not to be expected, which is confirmed by the sieving analysis of the bottom ashes, Figure 11. The use of halloysite caused an increased formation of quartz and K-Al silicates (WLR and WCB). In addition, Ca-Al silicates as well as  $\text{Fe}_2\text{O}_3$ ,  $\text{MgO}$  and  $\text{PbO}$  were determined for WCB. However, this cannot explain the increased proportion of sintering in the furnace ash when halloysite is used, as these phases have a relatively high melting point ( $>1500^\circ\text{C}$  [111]). Probably the interaction of the individual (crystalline and amorphous) phases causes a reduction of the ash melting point.

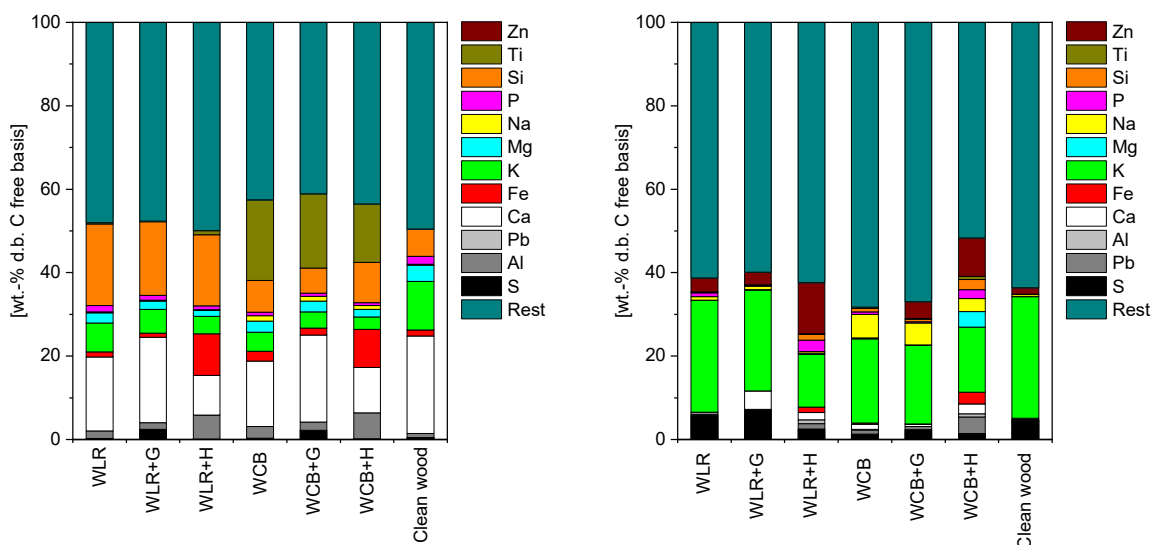


Figure 12: Analysis of the bottom ash, left, and total particulate matter, right, from the combustion of WLR and WCB pellets with additives. (WLR: wood logging residues, WCB: residues from chipboard processing, G: gypsum, H: halloysite, Clean Wood: ENplus wood pellets / class A1)

The composition of the total particulate matter is shown in Figure 12 (right). The use of gypsum has demonstrated a higher proportion of S in the particulate matter, which could lead to a significant shift from chlorides to sulphates in the particulate matter and indicates a lower risk of corrosion, Figure 12 (right) [60]. Unfortunately, the chloride content in the flue dust particles could not be determined due to the small amount of the available sample. In the case of WLR+G, some coarse particles may have been released, as the relative proportion of Ca is higher than in the combustion of pure WLR pellets. In addition, the combustion of WLR and WCB with halloysite has always increased the proportion of Si, Fe and Ca in the particles, indicating a higher proportion of coarse particles entrained from the firebed. A significant share of Pb and Zn was also found in particulate matter, since both elements are volatile during combustion and are contained in a higher share in the fuels that were added with halloysite. In contrast, there is a reduced proportion of potassium in the particles from the combustion of WLR+H and WCB+H. The reduction is 53% and 23%, respectively, which could indicate a preferred integration of K into the furnace ash. This trend is also confirmed by the parameters K Enrichment (calculated according to [48]) and K Release (calculated according to [11]) derived from the analyses, Table 7.

Table 7: K Enrichment and K release from the combustion of additive WLR and WCB pellets (n.d. not determined).

Fuel	K Enrichment	K release
WLR	0.93	31.3
WLR+G	1.12	20.5
WLR+H	1.07	16.6
WCB	1.51	n.d.
WCB+G	1.79	n.d.
WCB+H	2.31	n.d.
Clean wood	0.78	57.4

The XRD analyses of the total particulate matter show that the particles from the combustion of the non-additive fuels essentially consist of chlorinated compounds (i.e. KCl and NaCl), Table 8. The use of gypsum increases the formation of sulphur-containing compounds ( $K_3Na(SO_4)_2$  and  $K_2SO_4$ ) and reduces the share of chlorinated compounds. In addition, it could also be shown that the presence of  $CaMgO_6$ ,  $CaSiO_3$ ,  $SiO_2$ ,  $CaCO_3$ ,  $Ca_2Mg[Si_2O_7]$  probably led to coarse particles being entrained into the flue gas when the additives were used. Although the chemical analysis has shown an increased share of Zn and Pb in the particles, especially when halloysite is used, traces of PbO could only be detected in WCB+H. It is likely that Zn and Pb compounds are increasingly found in the amorphous phase.

Table 8: XRD Analysis of the bottom ash and particulate matter from the combustion of WLR and WCB pellets with additives

Phase	Phase name	Bottom ash						Total particulate matter					
		WLR	WLR + G	WLR + H	WCB	WCB + G	WCB + H	WLR	WLR + G	WLR + H	WCB	WCB + G	WCB + H
KCl	Sylvite												
NaCl	Halite												
K <sub>3</sub> Na(SO <sub>4</sub> ) <sub>2</sub>	Aphthitalite												
K <sub>2</sub> SO <sub>4</sub>	Arcanite												
CaMgO <sub>6</sub>	Dolomite												
CaSiO <sub>3</sub>	Wollastonite												
SiO <sub>2</sub>	Quartz												
CaCO <sub>3</sub>	Calcite												
Ca <sub>2</sub> Mg[Si <sub>2</sub> O <sub>7</sub> ]	Akermanite												
Ca <sub>3</sub> Mg(SiO <sub>4</sub> ) <sub>2</sub>	Merwinite												
K <sub>2</sub> Mg <sub>2</sub> [SO <sub>4</sub> ] <sub>3</sub>	Langbeinite												
TiO <sub>2</sub>	Rutile												
K <sub>2</sub> Ca <sub>2</sub> (SO <sub>4</sub> ) <sub>3</sub>	Calciolangbeinite												
MgO	Periclase												
KAlSi <sub>2</sub> O <sub>6</sub>	Leucite												
PbO													
Ca <sub>2</sub> Al(AlSi)O <sub>7</sub>	Gehlenite												
Fe <sub>2</sub> O <sub>3</sub>	Hematite												
CaMg[CO <sub>3</sub> ] <sub>2</sub>	Dolomite												
Ca <sub>3</sub> Al <sub>2</sub> O <sub>6</sub>													
CaMg <sub>2</sub> [SO <sub>4</sub> ] <sub>3</sub>	Perkovaite												
	dominant crystalline phase >50% (DP)												
	major crystalline phase 10-50% (MaP)												
	minor crystalline phase 5-10% (MiP)												
	trace crystalline phase <5% (TP)												

## 2.3 Industrial-scale combustion tests

### 2.3.1 Implementation of additive dosing

For technical reasons, the existing Endress heating plants only allow the additives to be dosed into the fuel auger before the fuel is introduced into the combustion chamber. However, Endress existing dosing technology was characterized by a too high throughput. Therefore a dosing unit of the company Gericke available at the DBFZ was applied. The applicability of the dosing unit was tested for the two additives halloysite and gypsum for different configurations (i.e. size of the dosing spirals (S), dosing tubes (DR) and settings of the frequency converter (FU) in the range of 5-100%, Figure 13 and Figure 14). The dosing of halloysite was possible without any problems. In contrast, no continuous dosing operation and discharge from the storage tank could be achieved with gypsum, especially at low conveying rates. This was due to the agglomeration tendency of the additive, which leads to clumping and bridging. Various measures were tested, e.g. mixing with wood chips and screening the additive before dosage. Accordingly, the mixture with wood shavings (in a share of 30 wt.%, 40 wt.% and 50 wt.%, respectively) was tested as a countermeasure. However, due to the still existing agglomeration tendency of the gypsum, it was not possible to achieve continuous dosing operation here either. The Y1-1 agitator offered by Gericke reduced the agglomeration and bridging tendency of the gypsum in the storage tank so that continuous dosing was possible.

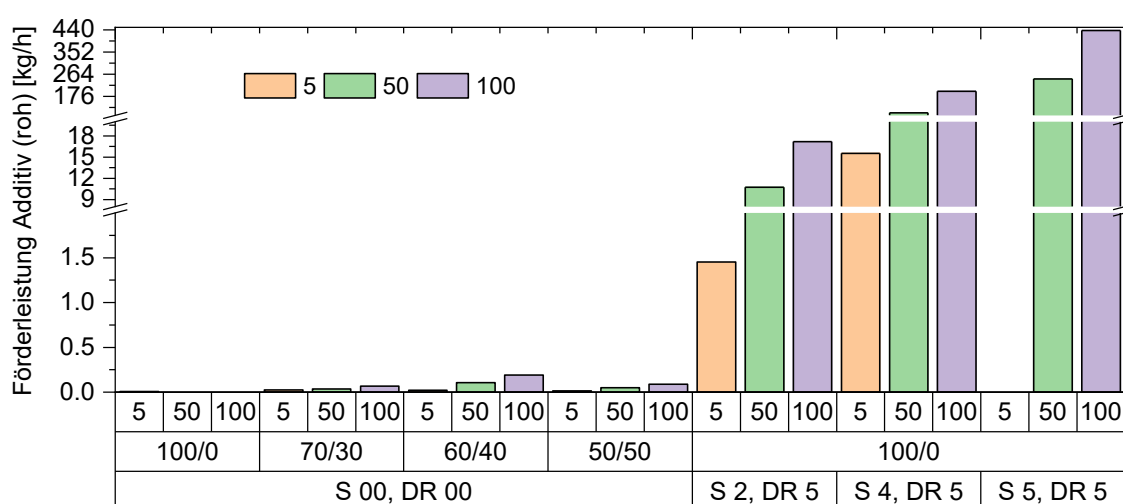


Figure 13: Gypsum throughput for the mixtures 100/0, 70/30, 60/40 and 50/50 (additive/wood shavings) for the GERICKE GLD87 dosing unit with a capacity of 5%, 50% and 100% (S: dosing spiral; DR: dosing tube).

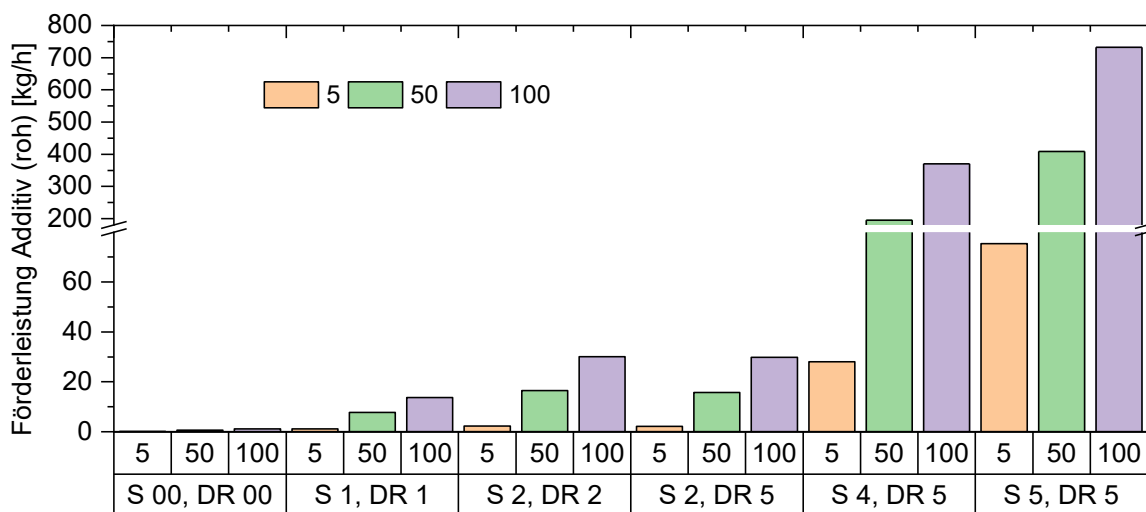


Figure 14: Halloysite throughput for the GERICKE GLD87 dosing unit with a capacity of 5%, 50% and 100% (S: dosing spiral; DR: dosing tube).

The mass throughput of halloysite and gypsum was then recorded with this system configuration, Figure 15. In the operation range of the FI between 5% and 100%, a linear dosing characteristic was obtained, whereby significantly more halloysite can be conveyed compared to gypsum for the same system configuration due to the higher bulk density. The characteristic curves were used to adjust the additive dosing performance during the combustion tests on industrial scale. Depending on the load condition and fuel throughput, the required additive quantity can thus be adjusted.

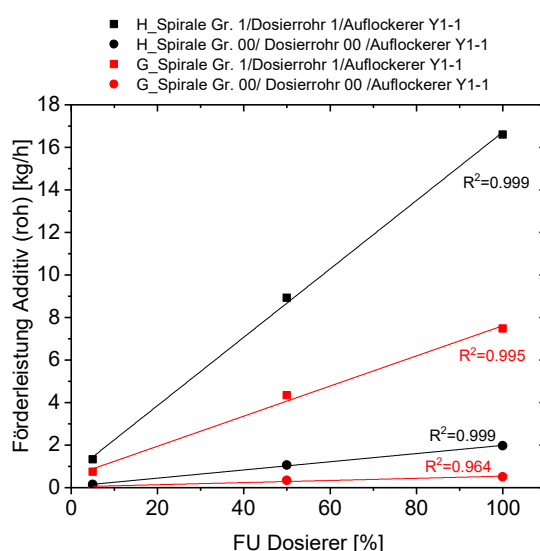


Figure 15: Throughput rate of the GERICKE GLD87 dosing unit for the use of gypsum and halloysite using the the 1-1 agitator

## 2.3.2 Combustion tests

For the WLR and WCB fuels used in the combustion tests on industrial scale, new batches were purchased from the same fuel suppliers (Chapter 1.1) due to organizational issues. The fuel analysis for the WLR and WCB fuels used in the industrial field tests is shown in Table 9. Compared to the pelletized materials used in the small combustion plant, WLR had a lower ash and nitrogen content and a chlorine and sulphur content twice as high. The lower ash content is caused in particular by a significantly lower silicon content, while the other main ash forming elements (e.g. K, Ca, Mg) are at a comparable level. In contrast, the WCB batch had similar properties to the pelletized materials used in the small combustion appliance. Slightly higher contents were determined for Ca, K and Ti and a lower Si content were determined. Compared to the pelletized batches, the fuel indices listed in Table 9 are lower for WLR and higher for WCB (with the exception of 2S/Cl).

Table 9: Fuel properties for WLR and WCB when used in the Endress combustion plant, type USF-W 800 (WLR: wood logging residues, WCB: residues from chipboard processing, n.n. not detectable)

Parameter	Unit	WLR	WCB
Water content	wt.-%	8.33	6.75
Lower heating value	MJ/kg d.b.	19.13	18.63
Ash content	wt.-% d.b.	1.52	1.75
N	wt.-% d.b.	0.32	4.33
S	wt.-% d.b.	0.027	0.023
Cl	wt.-% d.b.	0.090	0.030
Al	mg/kg d.b.	374	538
Pb	mg/kg d.b.	n.n.	8.8
Cd	mg/kg d.b.	0.2	0.2
Ca	mg/kg d.b.	4290	2870
Cr	mg/kg d.b.	2.93	5.7
Fe	mg/kg d.b.	203	294
K	mg/kg d.b.	1860	755
Cu	mg/kg d.b.	2.67	7.8
Mg	mg/kg d.b.	530	460
Mn	mg/kg d.b.	392	231
Na	mg/kg d.b.	46.1	268
Ni	mg/kg d.b.	1.78	1.5
P	mg/kg d.b.	409	212
Si	mg/kg d.b.	2500	1840
Ti	mg/kg d.b.	10.8	1740
Zn	mg/kg d.b.	30,.	48.1
(K+Na)/(2S+Cl)	mol/mol	2,6	1.35
Si/(Ca+Mg)	mol/mol	0.9	0.72
(Si+P+K)/(Ca+Mg)	mol/mol	1.16	1.01
Si/K	mol/mol	1.78	3.39
2S/Cl	mol/mol	6.63	1.72

Under the assumption that the additives are completely inert, the theoretically expected values for ash, S, Ca, Si, Al, Fe, Mg can be calculated on the basis of the analysis values and the admixing rates



for the additives (chapters 1.1 and 2.1) for the additivated fuel batches, Table 10. The addition of both additives increased the ash content in the fuels. The addition of gypsum led to increased contents of Ca and S in the fuel. In contrast, Al, Fe and Si were significantly increased by using hallosite as an additive. The content of K and Mg remained mainly unchanged. This trend is also reflected in the fuel indices. Thus, Si/(Ca+Mg), Si/K were highest for fuels that were added with halloysite, indicating a higher risk of slag formation in the furnace. The addition of gypsum mainly affected the 2S/Cl ratio.

Table 10: Calculated fuel properties for the additive admixture in the combustion of WLR and WCB in the Endress combustion plant, type USF-W 800

Parameter	Unit	Calculated values for additive admixture			
		WLR+G	WLR+H	WCB+G	WCB+H
ash content	wt.-% d.b.	2.84	3.07	2.17	2.79
S	wt.-% d.b.	0.254	0.027	0.096	0.024
Al	mg/kg d.b.	401	2470	546	2200
Ca	mg/kg d.b.	7520	4300	3910	2890
Fe	mg/kg d.b.	221	2400	299	2030
K	mg/kg d.b.	1850	1840	756	747
Mg	mg/kg d.b.	564	555	472	481
Si	mg/kg d.b.	2650	4540	1889	3460

Under full load conditions, the comparison of the set and measured values of the added additive quantity showed acceptable values:

- WLR+G (set: 25 g/min, measured: 24 g/min)
- WLR+H (set: 95 g/min, measured: 78 g/min)
- WCB+G (set: 13,8 g/min, measured: 8,8 g/min)
- WCB+H (set: 31,7 g/min, measured: 27 g/min)

Differences can occur due to measurement deviations during backweighing, material losses and deviating flow behavior of the additives in the dosing unit as well as assumptions in the calculation of the set values (bulk density, quality of the dosing characteristics). As described in Section 1.3, the combustion plant could be operated for max. 1.5 h under steady-state full load conditions due to the infrastructural conditions. During the stationary test operation, the average CO emissions from the combustion of all fuels were at a low level ( $<100 \text{ mg/m}^3$ ), Figure 16. The average NO<sub>x</sub> emissions ranged from 165 mg/m<sup>3</sup> for WLR to about 600 mg/m<sup>3</sup> for WCB, WCB+G and WCB+H batches. The emission values correspond to the findings known from the literature [26, 89-94]. Differences in NO<sub>x</sub> emissions are mainly due to the nitrogen content of the fuel. The emissions from the industrial combustion tests are significantly lower than those from the small combustion plant (Section 2.2). This may be due to the differences in the fuel nitrogen content of the fuels used as well as to the different firing principles and the exhaust gas recirculation used in industrial combustion plant. The combustion of fuels with a high S content led to higher SO<sub>2</sub> emissions. The combustion of the WLR and WCB batches without additives was characterized by a similarly low SO<sub>2</sub> emission level of  $< 21 \text{ mg/m}^3$ . However, the use of gypsum as an additive led to very high S contents in the fuel and thus also to the highest SO<sub>2</sub> emissions of 155mg/m<sup>3</sup> for WLR+G. As suggested by Rebbling et al. [60], elevated SO<sub>2</sub> values resulting from the degradation of CaSO<sub>4</sub> are likely. HCl emissions are at a low level of max. 8.4 mg/m<sup>3</sup>. In this context, the HCl emissions of WLR are lower than those of WCB combustion. The use

of gypsum and halloysite as additives led to higher HCl emissions during combustion in both WLR and WCB. The increased HCl emissions from the use of halloysite are also confirmed by test results with the pelleted material in the small combustion plant (Chapter 2.2) and tests with the additive kaolin, which has a similar material composition and effect to halloysite [30, 32, 34, 96]. In contrast, the highest HCl emissions were measured when gypsum was used. This was also observed in Rebbing et al. during the combustion of reed grass, wheat straw and bark, where a reduced formation of salty particles in the flue gas was suspected [60].

The average total particulate matter emissions (TPM) were between 49 and 129 mg/m<sup>3</sup>. The highest TPM emissions were found during the combustion of WCB. The use of halloysite reduced TPM emissions only in the case of WCB. This may have been caused by the increased retention of potassium in the bottom ash [30, 32-34, 63, 79, 97]. In contrast, this effect could not be demonstrated with WLR. This probably results from the TPM measuring method used with Wöhler SM500, which requires a significantly higher measurement uncertainty, Chapter 1.3.

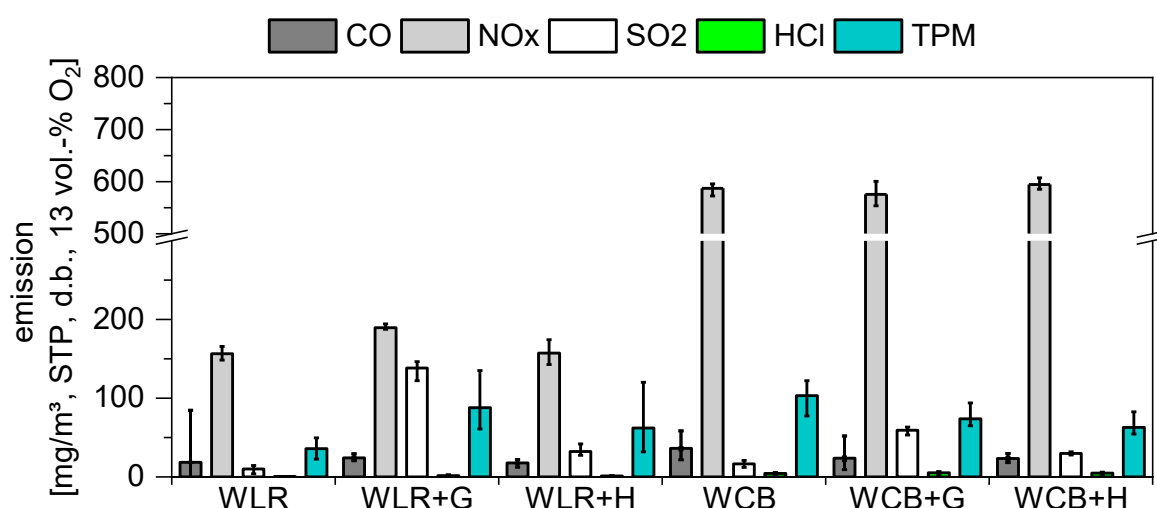


Figure 16: Emissions during combustion of WLR and WCB with and without addition of additives in the Endress combustion plant, type USF-W 800.

Based on the fuel indices, an increased risk of slagging in the combustion chamber ash was expected for the use of halloysite. Compared to the raw material used in the combustion tests in the small combustion plant, the WLR charge used in the industrial combustion tests had fewer critical properties with regard to the sintering to be expected in the bottom ash, Table 9. Accordingly, no significant sintering in the bottom ash could be obtained for this and the other fuels (except for WCB+H). In addition, the sintering at WCB+H occurred to a lesser extent in comparison to the experiments in the small combustion plants, which can presumably be attributed to the exhaust gas recirculation into the firebed and the associated limitation of the firebed temperature.



Figure 17: Ash agglomerates in the bottom ash during the combustion of WCB+H in the Endress combustion plant, type USF-W 800.

The elements in the bottom ashes show a very similar characteristic as the bottom ashes from the combustion in the small combustion appliance, see Figure 12 (left) and Figure 18. The main ash forming elements in the bottom ashes from the combustion of the WLR and WCB batches without additives were Si, K and Ca. However, a significant higher share of Si was found in the bottom ashes from the combustion of the WCB fuels in the industrial combustion plant. This can be attributed to the higher Si content in the applied WCB batch. During combustion tests on industrial scale, the use of gypsum also increased the Ca and S content while the use of halloysite increased the Fe and Al concentration in the bottom ash. The crystalline phase consists in the bottom ash from the combustion of WLR consisted to a large extent of  $\text{SiO}_2$ , Table 11. Due to the differences in the raw material composition with a significantly lower Si content compared to the calcium content, a large share of  $\text{CaMgO}_6$ ,  $\text{CaCO}_3$  and  $\text{Ca}_3\text{SiO}_5$  are also found in the bottom ash. The addition of additives to WLR did not result in further dominant phases. The expected retention of potassium in the bottom ash by the addition of halloysite is not confirmed by the crystalline ash fractions. During the combustion of WCB, the crystalline phase of the bottom ash is dominated by  $\text{SiO}_2$  and  $\text{K}_2\text{Ca}_2(\text{SO}_4)_3$ . Due to the high Ti content in the fuel, considerable amounts of  $\text{TiO}_2$  can be found. The phases in the furnace ash from the combustion of WCB change only insignificantly due to the addition of additives. However, additional phases of  $\text{KAlSi}_2\text{O}_6$  and  $\text{Ca}_3\text{Al}_2\text{O}_6$  can also be found in the slag. Overall, the increased tendency to slagging during the combustion of WCB+H is not reflected in the crystalline composition of the furnace ash. The reduction of the ash melting point is therefore probably due to the interaction of crystalline and amorphous phases.

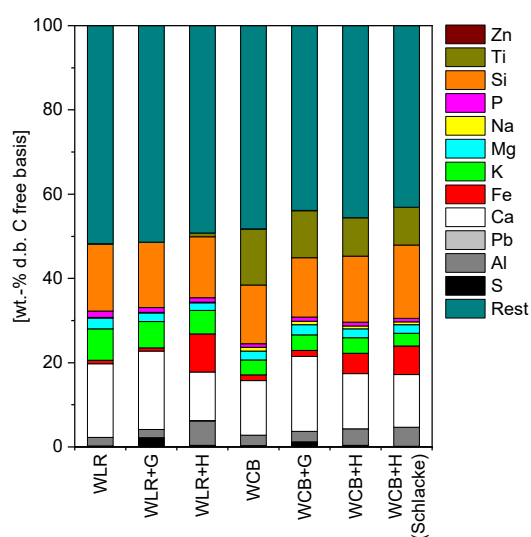


Figure 18: Analysis of the bottom ash from the combustion of WLR and WCB batches with additives in the Endress combustion plant, type USF-W 800 (WLR: wood logging residues, WCB: residues from chipboard processing, G: gypsum, H: halloysite).

Furthermore, the composition of the cyclone ash and the particulate matter from the combustion of WCB was investigated, Table 11 and Figure 19. The addition of additives is mainly reflected in the particulate matter composition. A reduction of the NaCl content was observed for both additives, Table 11. For gypsum,  $K_2SO_4$  is apparent as an additional phase. When halloysite is used  $Ca_2Mg[Si_2O_7]$ ,  $MgCO_3$  and  $CaMg(CO_3)_2$  are found as dominant phases in the particulate matter. However, this is probably due to the increased entrainment of coarse particles in the flue gases. The cyclone ash from the combustion of WCB, WCB+G and WCB+H mainly contains high-melting compounds such as  $SiO_2$ ,  $CaCO_3$ ,  $Ca_3MgO_8Si_2$ ,  $CaO$  and  $Ca_3SiO_5$ . If one considers the elementary composition of the bottom and cyclone ashes as well as the particulate matter (Figure 19) from the combustion of WCB, the Ti content of the combustion chamber ashes is first noticeable. This can be traced back to paintings and coatings in the fuel [110]. The cyclone ash also contains considerable amounts of Ti, Si, Ca and Mg, which indicates that coarse particles are entrained in the flue gas. K, Cl and S can only be found to a small extent in the cyclone ash, but increasingly in the total particulate matter. Since the addition of additives led to a reduction in TPM emissions overall, the proportion of K in fine dust increased compared with combustion without additives. As expected, the S content in the fine dust particles is highest through the use of gypsum, which could lead to a shift from chlorides to sulphates in the particulate material and indicates a lower corrosion risk [60]. However, the chlorine content is still high. In this context, the possibility of chemical reactions are determined by the concentrations of the individual substances and their thermodynamic equilibria. However, the equilibria are usually not reached due to temperature gradients which change locally and over time and because many reactions are too slow compared to the available residence times. Accordingly, sulphation can generally only significantly be expected in the upstream flue gas section. Due to the low reaction rate, it is hardly possible to achieve extensive sulphation by  $SO_2$  in the course of the downstream flue gas section. In a biomass-fired boiler, in which the gas residence time is typically only a few seconds,  $SO_3$  is required as far as possible due to the rapid reaction in order to achieve rapid sulphation of alkali chlorides [112]. However, the homogeneous oxidation of  $SO_2$  to  $SO_3$  is rather slow under boiler conditions, since the reaction is thermodynamically limited at high temperatures (e.g.  $>1100^\circ C$ ) and kinetically limited at low temperatures (e.g.  $<900^\circ C$ ) [112-114]. These interactions could be shown experimentally in the

combustion of wood chips and by simulations of the chemical reactions for different sulfur-containing additives [115].

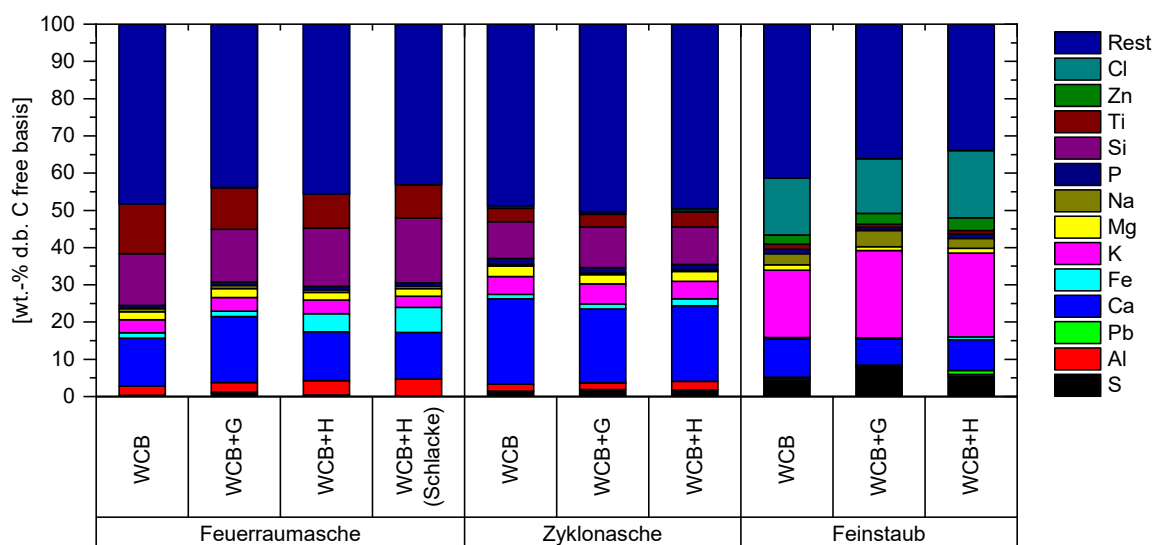


Figure 19: Analysis of the bottom ash, cyclone ash and total particulate matter from the combustion of the pure and additivated WCB batch in the Endress combustion plant, type USF-W 800 (WLR: wood logging residues, WCB: residues from chipboard processing, G: gypsum, H: halloysite). For methodological reasons, it was not possible to analyze Si in the particulate matter.

In order to evaluate the utilization of the bottom ashes as fertilizer, an analysis according to the German DüMV [116] was performed by an external laboratory. The results of the analysis are summarized in Table 12. On the basis of the results only the limit values for Ni (WCB+H) and Cr<sup>VI</sup> (WCB, WCB+H) could not be kept. However, the combustion chamber ashes cannot be declared due to the origin of the fuel (residues from chipboard processing), since the DüMV prescribes the use of untreated wood for the production of wood ashes.

Table 11: XRD Analysis of bottom ash, cyclone ash and total particulate matter from the combustion of the pure and addivated WLR and WCB in the Endress combustion plant, type USF-W 800 (WLR: wood logging residues, WCB: residues from chipboard processing, G: gypsum, H: halloysite)

[illegible]

Table 12: Analysis of bottom ash, cyclone ash and total particulate matter from the combustion of the pure and addivated WLR and WCB in the Endress furnace, type USF-W 800 according to DüMV. (WCB: residues from chipboard processing, G: gypsum, H: halloysite, n.b.: not calculated since all values are < BG, BG: limit of determination).

Parameter	Unit	General limit values DüMV	Limit values for forestry land	WCB	WCB+G	WCB+H
Dry matter	wt.%			99.8	100.0	99.8
pH value				12.5	12.5	12.3
pH in CaCl <sub>2</sub>				12.5	12.5	12.5
Reactivity	%			80.9	72.8	62.0
Conductivity	µs/cm			10000	12900	8080
Salinity	mg/100g OS			5280	6810	4270
Basic active substances	% CaO			21.7	26.5	20.2
Ammonium	mg/kg d.b.			0.98	0.58	1.2
Total nitrogen	wt.%			< 0.05	< 0.05	0.06
Arsenic (As)	mg/kg d.b.	40	60	< 0.8	< 0.8	9.5
Lead (Pb)	mg/kg d.b.	150	225	21	14	21
Boron (B)	mg/kg d.b.			210	209	197
Cadmium (Cd)	mg/kg d.b.	1.5	2.25	0.4	0.9	0.4
Calcium (Ca)	mg/kg d.b.			126000	143000	118000
Chrome (Cr)	mg/kg d.b.			136	82	139
Cobalt (Co)	mg/kg d.b.			11	10	81
Iron (Fe)	mg/kg d.b.			9990	8990	37900
Potassium (K)	mg/kg d.b.			23500	26600	33500
Copper (Cu)	mg/kg d.b.			474	314	509
Magnesium (Mg)	mg/kg d.b.			17900	18300	18700
Sodium (Na)	mg/kg d.b.			6720	5910	6140
Nickel (Ni)	mg/kg d.b.	80	120	43	37	127
Phosphorus (P)	mg/kg d.b.			3620	4170	9250
Mercury (Hg)	mg/kg d.b.	1	1.5	< 0.07	< 0.07	< 0.07
sulphur	mg/kg d.b.			1750	6010	2720
Selenium (Se)	mg/kg d.b.			< 1	< 1	< 1
Thallium (Tl)	mg/kg d.b.	1	1.5	< 0.2	< 0.2	< 0.2



Zinc (Zn)	mg/kg d.b.			351	278	365
Chrome VI (Cr <sup>VI</sup> )	mg/kg d.b.	2		34.4	< 0.5	8.9
ignition loss	wt.% d.b.			0.5	0.6	3.1
Sum PFOS / PFOA excl. BG	µg/kg d.b.	0.1	0.15	n.b.	n.b.	n.b.
Total PCDD/F + dl-PCB (WHO-TE 2005 incl. BG)	µg/kg	30		0.004	0.004	0.006
Screen passage 6.3 mm	wt. %			100	100	100
Screen passage 3.15 mm	wt. %			100	100	100



## 2.4 Conclusions

The following conclusion can be drawn on the basis of the performed experiments:

### **Pelletization of fuels with additives**

The pelletization of WLR generally requires a higher specific energy input than the pelleting of WCB. During the pelleting of WCB, the adhesive present in the WCB hardens in combination with water under the prevailing temperatures, whereby the frictional forces in the die could be reduced by a higher input water content. The addition of halloysite reduced the specific energy input for pelleting, both for WLR and WCB. In summary, however, it was shown that the pelleting of WCB and WLR with and without additives is still challenging in order to meet the requirements of DIN EN ISO 17225-2. There is a need for further research with regard to the optimal raw material and plant parameters.

### **Effect of additives on combustion**

Although the addition of halloysite had advantages for pelleting and a reduction of total particulate matter (> 40%) in the flue gas could be achieved, the increase in ash content and the risk of slagging in the bottom ash appear to be a major challenge for wood combustion. The reduction potential of Cl-containing particles combined with high SO<sub>2</sub> emissions could be demonstrated by the use of gypsum as an additive. However, the sulphation reactions (i.e. the effectiveness of the gypsum additive) appear to be rather limited under the prevailing boiler conditions. Accordingly, care must be taken to use additives that are as uncontaminated as possible and to determine the quantities of additives to be used simply but sufficiently. Thus, the use of halloysite and gypsum should be limited to fuel ranges with a high K and Cl content. The bottom ashes cannot be declared as fertilizer.

### **Additive dosing**

Additive dosing was successfully implemented in the fuel auger of the industrial combustion plant. No significant differences in the emission and ash behavior between this type of additive addition and the admixture during pelleting could be determined. Depending on the firing principle, there may be an increased risk of particle discharge (e.g. as non-converted additive) from the combustion chamber. Additive dosing into fuel auger requires an additive characteristic that is as homogeneous and constant as possible (bulk density, particle size distribution) and suitable for the applied dosing device. With recycled gypsum, prior separation of coarse particles can be helpful. In addition, the throughput rates should be determined individually for the additive to be used.

## 3 Knowledge from third parties during project duration

During the project period, a scientific publication on combustion with the addition of recycled gypsum in a 20 kW (underfeed furnace for wood pellets) and 40 MW furnace (grate furnace) became known for the implementation of the joint project [60]. In this publication, cereal straw, reed canary gras, municipal waste and bark were used. It should be noted that the furnace ash in the 40 MW furnace was actively cooled in the ash discharge, which makes it difficult to compare the results in the publication. Further studies investigated the use of kaolin with sawdust from wood [63], sunflower

husks [97], wheat straw (e.g. mixed with wood) [34], poplar [34], hay [34], short rotation wood [32], olive press cake [30, 63]. Studies have also shown that kaolinite was used in the combustion of beech wood chips [33, 96]. In these investigations, a reduction in dust emissions and an increase in ash melting temperatures with the formation of high-melting K-Al silicates were observed. At the same time, the proportion of K in the deposits and fine dust decreases and the risk of increased SO<sub>2</sub> and HCl emissions increases. In [63] it became clear that the use of kaolin in clean wood fuels is not sensible and should be limited to fuels rich in potassium and chlorine. In addition, the particle size seems to have an influence on the reaction with potassium [39, 40]. In contrast, far fewer studies were known to investigate the use of halloysite [79, 97]. The results show similar behavior to that of kaolin and kaolinite [79], with the effect of halloysite not appearing to be more efficient than that of kaolin [97]. Studies on particle deposition rates and their characteristics in the heat transfer surfaces of small combustion plants were not known at the beginning of the project. During the project a study on the experimental [117] and numerical [118] determination of deposition rates became known.

No patent applications have become known.

## References

1. Wang L, Hustad JE, Skreiberg Ø et al. (2012) A Critical Review on Additives to Reduce Ash Related Operation Problems in Biomass Combustion Applications. *Energy Procedia* 20: 20–29. doi: 10.1016/j.egypro.2012.03.004
2. Niu Y, Tan H, Hui S'e (2016) Ash-related issues during biomass combustion: Alkali-induced slagging, silicate melt-induced slagging (ash fusion), agglomeration, corrosion, ash utilization, and related countermeasures. *Progress in Energy and Combustion Science* 52: 1–61. doi: 10.1016/j.pecs.2015.09.003
3. Gollmer C, Höfer I, Kaltschmitt M (2018) Additives as a fuel-oriented measure to mitigate inorganic particulate matter (PM) emissions during small-scale combustion of solid biofuels. *Biomass Conv. Bioref.* 20(5): 20. doi: 10.1007/s13399-018-0352-4
4. van Loo S (ed) (2010) *The handbook of biomass combustion and co-firing*, Paperback [ed.]. Biomass. Earthscan, London u.a.
5. Glarborg P (2007) Hidden interactions—Trace species governing combustion and emissions. *Proceedings of the Combustion Institute* 31(1): 77–98. doi: 10.1016/j.proci.2006.08.119
6. Vassilev SV, Baxter D, Andersen LK et al. (2010) An overview of the chemical composition of biomass. *Fuel* 89(5): 913–933. doi: 10.1016/j.fuel.2009.10.022
7. Zevenhoven M, Yrjas P, Skrifvars B-J et al. (2012) Characterization of Ash-Forming Matter in Various Solid Fuels by Selective Leaching and Its Implications for Fluidized-Bed Combustion. *Energy Fuels* 26(10): 6366–6386. doi: 10.1021/ef300621j
8. Pollex A, Zeng T, Khalsa J et al. (2018) Content of potassium and other aerosol forming elements in commercially available wood pellet batches. *Fuel* 232: 384–394. doi: 10.1016/j.fuel.2018.06.001
9. Kaltschmitt M, Hartmann H, Hofbauer H (2016) *Energie aus Biomasse: Grundlagen, Techniken und Verfahren*, 3rd edn. Springer, Berlin, Heidelberg
10. Obernberger I, Brunner T, BARNTHALER G (2006) Chemical properties of solid biofuels—significance and impact. *Biomass and Bioenergy* 30(11): 973–982. doi: 10.1016/j.biombioe.2006.06.011
11. Sommersacher P, Brunner T, Obernberger I (2012) Fuel Indexes: A Novel Method for the Evaluation of Relevant Combustion Properties of New Biomass Fuels. *Energy Fuels* 26(1): 380–390. doi: 10.1021/ef201282y
12. Knudsen JN, Jensen PA, Dam-Johansen K (2004) Transformation and Release to the Gas Phase of Cl, K, and S during Combustion of Annual Biomass. *Energy Fuels* 18(5): 1385–1399. doi: 10.1021/ef049944q

13. Bäfver LS, Rönnbäck M, Leckner B et al. (2009) Particle emission from combustion of oat grain and its potential reduction by addition of limestone or kaolin. *Fuel Processing Technology* 90(3): 353–359. doi: 10.1016/j.fuproc.2008.10.006
14. Boström D, Grimm A, Boman C et al. (2009) Influence of Kaolin and Calcite Additives on Ash Transformations in Small-Scale Combustion of Oat. *Energy Fuels* 23(10): 5184–5190. doi: 10.1021/ef900429f
15. Müller M, Wolf K-J, Smeda A et al. (2006) Release of K, Cl, and S Species during Co-combustion of Coal and Straw. *Energy Fuels* 20(4): 1444–1449. doi: 10.1021/ef0600356
16. Knudsen JN, Jensen PA, Lin W et al. (2004) Sulfur Transformations during Thermal Conversion of Herbaceous Biomass. *Energy Fuels* 18(3): 810–819. doi: 10.1021/ef034085b
17. Christensen KA, Stenholm M, Livbjerg H (1998) The formation of submicron aerosol particles, HCl and SO<sub>2</sub> in straw-fired boilers. *Journal of Aerosol Science* 29(4): 421–444. doi: 10.1016/S0021-8502(98)00013-5
18. Boman C, Nordin A, Boström D et al. (2004) Characterization of Inorganic Particulate Matter from Residential Combustion of Pelletized Biomass Fuels. *Energy Fuels* 18(2): 338–348. doi: 10.1021/ef034028i
19. van Lith SC, Alonso-Ramírez V, Jensen PA et al. (2006) Release to the Gas Phase of Inorganic Elements during Wood Combustion. Part 1: Development and Evaluation of Quantification Methods. *Energy Fuels* 20(3): 964–978. doi: 10.1021/ef050131r
20. van Lith SC, Jensen PA, Frandsen FJ et al. (2008) Release to the Gas Phase of Inorganic Elements during Wood Combustion. Part 2: Influence of Fuel Composition. *Energy Fuels* 22(3): 1598–1609. doi: 10.1021/ef060613i
21. Björkman E, Strömberg B (1997) Release of Chlorine from Biomass at Pyrolysis and Gasification Conditions 1. *Energy Fuels* 11(5): 1026–1032. doi: 10.1021/ef970031o
22. Dayton DC, French RJ, Milne TA (1995) Direct Observation of Alkali Vapor Release during Biomass Combustion and Gasification. 1. Application of Molecular Beam/Mass Spectrometry to Switchgrass Combustion. *Energy Fuels* 9(5): 855–865. doi: 10.1021/ef00053a018
23. Dayton DC, Jenkins BM, Turn SQ et al. (1999) Release of Inorganic Constituents from Leached Biomass during Thermal Conversion. *Energy Fuels* 13(4): 860–870. doi: 10.1021/ef980256e
24. Jensen PA, Frandsen FJ, Dam-Johansen K et al. (2000) Experimental Investigation of the Transformation and Release to Gas Phase of Potassium and Chlorine during Straw Pyrolysis. *Energy Fuels* 14(6): 1280–1285. doi: 10.1021/ef000104v
25. Johansen JM, Aho M, Paakkinen K et al. (2013) Release of K, Cl, and S during combustion and co-combustion with wood of high-chlorine biomass in bench and pilot scale fuel beds. *Proceedings of the Combustion Institute* 34(2): 2363–2372. doi: 10.1016/j.proci.2012.07.025

26. Tissari J, Sippula O, Kouki J et al. (2008) Fine Particle and Gas Emissions from the Combustion of Agricultural Fuels Fired in a 20 kW Burner. *Energy Fuels* 22(3): 2033–2042. doi: 10.1021/ef700766y
27. WEI X, Schnell U, HEIN K (2005) Behaviour of gaseous chlorine and alkali metals during biomass thermal utilization. *Fuel* 84(7-8): 841–848. doi: 10.1016/j.fuel.2004.11.022
28. Arvelakis S, Jensen PA, Dam-Johansen K (2004) Simultaneous Thermal Analysis (STA) on Ash from High-Alkali Biomass. *Energy Fuels* 18(4): 1066–1076. doi: 10.1021/ef034065
29. Knudsen JN, Jensen PA, Lin W et al. (2005) Secondary Capture of Chlorine and Sulfur during Thermal Conversion of Biomass. *Energy Fuels* 19(2): 606–617. doi: 10.1021/ef049874n
30. Batir O, Selçuk N, Kulah G (2018) Effect of kaolin addition on alkali capture capability during combustion of olive residue. *Combustion Science and Technology* 191(1): 43–53. doi: 10.1080/00102202.2018.1452376
31. Davidsson KO, Steenari B-M, Eskilsson D (2007) Kaolin Addition during Biomass Combustion in a 35 MW Circulating Fluidized-Bed Boiler. *Energy Fuels* 21(4): 1959–1966. doi: 10.1021/ef070055n
32. Gehrig M, Wöhler M, Pelz S et al. (2019) Kaolin as additive in wood pellet combustion with several mixtures of spruce and short-rotation-coppice willow and its influence on emissions and ashes. *Fuel* 235: 610–616. doi: 10.1016/j.fuel.2018.08.028
33. Huelsmann T, Mack R, Kaltschmitt M et al. (2018) Influence of kaolinite on the PM emissions from small-scale combustion. *Biomass Conversion and Biorefinery*. doi: 10.1007/s13399-018-0316-8
34. Mack R, Kuptz D, Schön C et al. (2019) Combustion behavior and slagging tendencies of kaolin additivated agricultural pellets and of wood-straw pellet blends in a small-scale boiler. *Biomass and Bioenergy* 125: 50–62. doi: 10.1016/j.biombioe.2019.04.003
35. Sommersacher P, Brunner T, Obernberger I et al. (2013) Application of Novel and Advanced Fuel Characterization Tools for the Combustion Related Characterization of Different Wood/Kaolin and Straw/Kaolin Mixtures. *Energy Fuels* 27(9): 5192–5206. doi: 10.1021/ef400400n
36. Steenari B-M, Karlfeldt Fedje K (2010) Addition of kaolin as potassium sorbent in the combustion of wood fuel – Effects on fly ash properties. *Fuel* 89(8): 2026–2032. doi: 10.1016/j.fuel.2010.02.006
37. Steenari B-M, Lindqvist O (1998) High-temperature reactions of straw ash and the anti-sintering additives kaolin and dolomite. *Biomass and Bioenergy* 14(1): 67–76. doi: 10.1016/S0961-9534(97)00035-4

38. Tran K-Q, Lisa K, Steenari B-M et al. (2005) A kinetic study of gaseous alkali capture by kaolin in the fixed bed reactor equipped with an alkali detector. *Fuel* 84(2–3): 169–175. doi: 10.1016/j.fuel.2004.08.019
39. Wang G, Jensen PA, Wu H et al. (2018) Potassium Capture by Kaolin, Part 2: K<sub>2</sub>CO<sub>3</sub>, KCl and K<sub>2</sub>SO<sub>4</sub>. *Energy Fuels*. doi: 10.1021/acs.energyfuels.7b04055
40. Wang G, Jensen PA, Wu H et al. (2018) Potassium Capture by Kaolin, Part 1: KOH. *Energy Fuels* 32(2): 1851–1862. doi: 10.1021/acs.energyfuels.7b03645
41. Zeng T, Pollex A, Weller N et al. (2018) Blended biomass pellets as fuel for small scale combustion appliances: Effect of blending on slag formation in the bottom ash and pre-evaluation options. *Fuel* 212: 108–116. doi: 10.1016/j.fuel.2017.10.036
42. Aho M, Paakkinen K, Taipale R (2013) Quality of deposits during grate combustion of corn stover and wood chip blends. *Fuel* 104: 476–487. doi: 10.1016/j.fuel.2012.05.057
43. Carroll JP, Finnan JM (2015) The use of additives and fuel blending to reduce emissions from the combustion of agricultural fuels in small scale boilers. *Biosystems Engineering* 129: 127–133. doi: 10.1016/j.biosystemseng.2014.10.001
44. Dragutinovic N, Höfer I, Kaltschmitt M (2019) Effect of additives on thermochemical conversion of solid biofuel blends from wheat straw, corn stover, and corn cob. *Biomass Conv. Bioref.* 9(1): 35–54. doi: 10.1007/s13399-017-0273-7
45. Fournel S, Palacios J, Godbout S et al. (2015) Effect of Additives and Fuel Blending on Emissions and Ash-Related Problems from Small-Scale Combustion of Reed Canary Grass. *Agriculture* 5(3): 561–576. doi: 10.3390/agriculture5030561
46. Lajili M, Jeguirim M, Kraiem N et al. (2015) Performance of a household boiler fed with agropellets blended from olive mill solid waste and pine sawdust. *Fuel* 153: 431–436. doi: 10.1016/j.fuel.2015.03.010
47. Lajili M, Limousy L, Jeguirim M (2014) Physico-chemical properties and thermal degradation characteristics of agropellets from olive mill by-products/sawdust blends. *Fuel Processing Technology* 126: 215–221. doi: 10.1016/j.fuproc.2014.05.007
48. Sippula O, Lamberg H, Leskinen J et al. (2017) Emissions and ash behavior in a 500 kW pellet boiler operated with various blends of woody biomass and peat. *Fuel* 202: 144–153. doi: 10.1016/j.fuel.2017.04.009
49. Zeng T, Kuptz D, Schreiber K et al. (2019) Impact of adhering soil and other extraneous impurities on the combustion and emission behavior of forest residue wood chips in an automatically stoked small-scale boiler. *Biomass Conv. Bioref.* 5(1): 35. doi: 10.1007/s13399-018-00368-z

50. Schön C, Kuptz D, Mack R et al. (2019) Influence of wood chip quality on emission behavior in small-scale wood chip boilers. *Biomass Conv. Bioref.* 9(1): 71–82. doi: 10.1007/s13399-017-0249-7
51. Lindström E, Öhman M, Backman R et al. (2008) Influence of Sand Contamination on Slag Formation during Combustion of Wood Derived Fuels. *Energy Fuels* 22(4): 2216–2220. doi: 10.1021/ef700772q
52. Steenari B-M, Lundberg A, Pettersson H et al. (2009) Investigation of Ash Sintering during Combustion of Agricultural Residues and the Effect of Additives. *Energy Fuels* 23(11): 5655–5662. doi: 10.1021/ef900471u
53. Paulrud S, Nilsson C, Öhman M (2001) Reed canary-grass ash composition and its melting behavior during combustion. *Fuel* 80(10): 1391–1398. doi: 10.1016/S0016-2361(01)00003-5
54. Näzelius I-L, Boström D, Rebbling A et al. (2017) Fuel Indices for Estimation of Slagging of Phosphorus-Poor Biomass in Fixed Bed Combustion. *Energy Fuels* 31(1): 904–915. doi: 10.1021/acs.energyfuels.6b02563
55. Lindström E, Larsson SH, Boström D et al. (2010) Slagging Characteristics during Combustion of Woody Biomass Pellets Made from a Range of Different Forestry Assortments. *Energy Fuels* 24(6): 3456–3461. doi: 10.1021/ef901571c
56. Llorente MF, Arocas PD, Nebot LG et al. (2008) The effect of the addition of chemical materials on the sintering of biomass ash. *Fuel* 87(12): 2651–2658. doi: 10.1016/j.fuel.2008.02.019
57. Schmitt VEM, Kaltschmitt M (2013) Effect of straw proportion and Ca- and Al-containing additives on ash composition and sintering of wood–straw pellets. *Fuel* 109: 551–558. doi: 10.1016/j.fuel.2013.02.064
58. Wang L, Skjevraak G, Hustad JE et al. (2012) Effects of Additives on Barley Straw and Husk Ashes Sintering Characteristics. *Energy Procedia* 20: 30–39. doi: 10.1016/j.egypro.2012.03.005
59. Xiong S, Burvall J, Örberg H et al. (2008) Slagging Characteristics during Combustion of Corn Stovers with and without Kaolin and Calcite. *Energy Fuels* 22(5): 3465–3470. doi: 10.1021/ef700718j
60. Rebbling A, Näzelius I-L, Piotrowska P et al. (2016) Waste Gypsum Board and Ash-Related Problems during Combustion of Biomass. 2. Fixed Bed. *Energy Fuels* 30(12): 10705–10713. doi: 10.1021/acs.energyfuels.6b01521
61. Fusco L de, Defoort F, Rajczyk R et al. (2016) Ash Characterization of Four Residual Wood Fuels in a 100 kW th Circulating Fluidized Bed Reactor Including the Use of Kaolin and Halloysite Additives. *Energy Fuels* 30(10): 8304–8315. doi: 10.1021/acs.energyfuels.6b01784



62. Öhman M, Nordin A (2000) The Role of Kaolin in Prevention of Bed Agglomeration during Fluidized Bed Combustion of Biomass Fuels. *Energy Fuels* 14(3): 618–624. doi: 10.1021/ef990198c
63. Roberts LJ, Mason PE, Jones JM et al. (2019) The impact of aluminosilicate-based additives upon the sintering and melting behavior of biomass ash. *Biomass and Bioenergy* 127: 105284. doi: 10.1016/j.biombioe.2019.105284
64. Thy P, Jenkins BM, Leshner CE et al. (2006) Compositional constraints on slag formation and potassium volatilization from rice straw blended wood fuel. *Fuel Processing Technology* 87(5): 383–408. doi: 10.1016/j.fuproc.2005.08.015
65. Fernández MJ, Mediavilla I, Barro R et al. (2019) Sintering reduction of herbaceous biomass when blended with woody biomass: Predictive and combustion tests. *Fuel* 239: 1115–1124. doi: 10.1016/j.fuel.2018.11.115
66. Sommersacher P, Brunner T, Obernberger I et al. (2015) Combustion related characterisation of Miscanthus peat blends applying novel fuel characterisation tools. *Fuel* 158: 253–262. doi: 10.1016/j.fuel.2015.05.037
67. Baxter LL, Miles TR, Jenkins BM et al. (1998) The behavior of inorganic material in biomass-fired power boilers: Field and laboratory experiences. *Fuel Processing Technology* 54(1): 47–78. doi: 10.1016/S0378-3820(97)00060-X
68. Jappe Frandsen F (2005) Utilizing biomass and waste for power production—a decade of contributing to the understanding, interpretation and analysis of deposits and corrosion products. *Fuel* 84(10): 1277–1294. doi: 10.1016/j.fuel.2004.08.026
69. Garcia-Maraver A, Mata-Sanchez J, Carpio M et al. (2017) Critical review of predictive coefficients for biomass ash deposition tendency. *Journal of the Energy Institute* 90(2): 214–228. doi: 10.1016/j.joei.2016.02.002
70. Åmand L-E, Leckner B, Eskilsson D et al. (2006) Deposits on heat transfer tubes during co-combustion of biofuels and sewage sludge. *Fuel* 85(10–11): 1313–1322. doi: 10.1016/j.fuel.2006.01.001
71. Elled AL, Davidsson KO, Åmand LE (2010) Sewage sludge as a deposit inhibitor when co-fired with high potassium fuels. *Biomass and Bioenergy* 34(11): 1546–1554. doi: 10.1016/j.biombioe.2010.05.003
72. Aho M, Yrjas P, Taipale R et al. (2010) Reduction of superheater corrosion by co-firing risky biomass with sewage sludge. *Fuel* 89(9): 2376–2386. doi: 10.1016/j.fuel.2010.01.023
73. Broström M, Kassman H, Helgesson A et al. (2007) Sulfation of corrosive alkali chlorides by ammonium sulfate in a biomass fired CFB boiler. *Fuel Processing Technology* 88(11–12): 1171–1177. doi: 10.1016/j.fuproc.2007.06.023

74. Jiménez S, Ballester J (2007) Formation of alkali sulphate aerosols in biomass combustion. *Fuel* 86(4): 486–493. doi: 10.1016/j.fuel.2006.08.005
75. Aho M, Vainikka P, Taipale R et al. (2008) Effective new chemicals to prevent corrosion due to chlorine in power plant superheaters. *Fuel* 87(6): 647–654. doi: 10.1016/j.fuel.2007.05.033
76. Piotrowska P, Rebbling A, Lindberg D et al. (2015) Waste Gypsum Board and Ash-Related Problems during Combustion of Biomass. 1. Fluidized Bed. *Energy Fuels* 29(2): 877–893. doi: 10.1021/ef5024753
77. Kalisz S, Ciukaj S, Mroczek K et al. (2015) Full-scale study on halloysite fireside additive in 230 t/h pulverized coal utility boiler. *Energy* 92, Part 1: 33–39. doi: 10.1016/j.energy.2015.03.062
78. Mroczek K, Kalisz S, Pronobis M et al. (2011) The effect of halloysite additive on operation of boilers firing agricultural biomass. *Fuel Processing Technology* 92(5): 845–855. doi: 10.1016/j.fuproc.2010.11.020
79. Plaza P, Maier J, Maj I et al. (2019) Potassium and chlorine distributions in high temperature halloysite formed deposits. *E3S Web Conf* 82. doi: 10.1051/e3sconf/20198201011
80. Paulrud S, Hjörnhede A, Öhman M (2015) Ready-made fuel mix of straw, wood chips and additive, from the terminal to the CHP-plant. *Aspects of Applied Biology* 131
81. Deutsches Institut für Normung (2014) DIN EN ISO 17225-4: Solid biofuels - Fuel specifications and classes - Part 4: Graded wood chips
82. Deutsches Institut für Normung (2002) DIN EN 13284-1: Stationary source emissions - Determination of low range mass concentration of dust - Part 1: Manual gravimetric method
83. VDI 2066-1 (2006) Particulate matter measurement - Dust measurement in flowing gases - Gravimetric determination of dust load
84. Deutsches Institut für Normung (2011) DIN EN 14780: Solid biofuels - Sample preparation
85. Deutsches Institut für Normung (2011) DIN EN 14778: Solid biofuels - Sampling
86. Deutsches Institut für Normung (2014) DIN EN ISO 17225-1: Solid biofuels - Fuel specifications and classes - Part 1: General requirements
87. Öhman M, Boman C, Hedman H et al. (2004) Slagging tendencies of wood pellet ash during combustion in residential pellet burners. *Biomass and Bioenergy* 27(6): 585–596. doi: 10.1016/j.biombioe.2003.08.016
88. Deutsches Institut für Normung (2003) DIN EN 12457-4: Characterization of waste - Leaching; Compliance test for leaching of granular waste materials and sludges - Part 4: One stage batch test at a liquid to solid ratio of 10 l/kg for materials with particle size below 10 mm (without or with limited size reduction)

89. Lamberg H, Tissari J, Jokiniemi J et al. (2013) Fine Particle and Gaseous Emissions from a Small-Scale Boiler Fueled by Pellets of Various Raw Materials. *Energy Fuels* 27(11): 7044–7053. doi: 10.1021/ef401267t
90. Carvalho L, Wopienka E, Pointner C et al. (2013) Performance of a pellet boiler fired with agricultural fuels. *Applied Energy* 104: 286–296. doi: 10.1016/j.apenergy.2012.10.058
91. Garcia-Maraver A, Zamorano M, Fernandes U et al. (2014) Relationship between fuel quality and gaseous and particulate matter emissions in a domestic pellet-fired boiler. *Fuel* 119: 141–152. doi: 10.1016/j.fuel.2013.11.037
92. Krugly E, Martuzevicius D, Puida E et al. (2014) Characterization of Gaseous- and Particle-Phase Emissions from the Combustion of Biomass-Residue-Derived Fuels in a Small Residential Boiler. *Energy Fuels* 28(8): 5057–5066. doi: 10.1021/ef500420t
93. Kortelainen M, Jokiniemi J, Nuutinen I et al. (2015) Ash behavior and emission formation in a small-scale reciprocating-grate combustion reactor operated with wood chips, reed canary grass and barley straw. *Fuel* 143: 80–88. doi: 10.1016/j.fuel.2014.11.006
94. Rabaçal M, Fernandes U, Costa M (2013) Combustion and emission characteristics of a domestic boiler fired with pellets of pine, industrial wood wastes and peach stones. *Renewable Energy* 51: 220–226. doi: 10.1016/j.renene.2012.09.020
95. Zeng T, Weller N, Pollex A et al. (2016) Blended biomass pellets as fuel for small scale combustion appliances: Influence on gaseous and total particulate matter emissions and applicability of fuel indices. *Fuel* 184: 689–700. doi: 10.1016/j.fuel.2016.07.047
96. Gollmer C, Höfer I, Harms D et al. (2019) Potential additives for small-scale wood chip combustion – Laboratory-scale estimation of the possible inorganic particulate matter reduction potential. *Fuel* 254: 115695. doi: 10.1016/j.fuel.2019.115695
97. De Fusco, L., Blondeau, J., Defoort, F., Jeanmart, H., Contino, F. (2016) Characterization of Sunflower Husks Fouling in a Drop Tube Furnace: Comparison of Deposits With H<sub>3</sub>PO<sub>4</sub>, CaCO<sub>3</sub> AND Al<sub>2</sub>Si<sub>2</sub>O<sub>5</sub>(OH)<sub>4</sub> Additives. In: *ETA-Florence Renewable Energies (ed) Proceedings of the 24th European Biomass Conference and Exhibition, Florence, Italy*, pp 748–755
98. Boström D, Skoglund N, Grimm A et al. (2012) Ash Transformation Chemistry during Combustion of Biomass. *Energy Fuels* 26(1): 85–93. doi: 10.1021/ef201205b
99. Lindström E, Sandström M, Boström D et al. (2007) Slagging Characteristics during Combustion of Cereal Grains Rich in Phosphorus. *Energy Fuels* 21(2): 710–717. doi: 10.1021/ef060429x
100. Sippula O, Lind T, Jokiniemi J (2008) Effects of chlorine and sulphur on particle formation in wood combustion performed in a laboratory scale reactor. *Fuel* 87(12): 2425–2436. doi: 10.1016/j.fuel.2008.02.004

101. Luan C, You C, Zhang D (2014) Composition and sintering characteristics of ashes from co-firing of coal and biomass in a laboratory-scale drop tube furnace. *Energy* 69: 562–570. doi: 10.1016/j.energy.2014.03.050
102. Niu Y, Zhu Y, Tan H et al. (2014) Investigations on biomass slagging in utility boiler: Criterion numbers and slagging growth mechanisms. *Fuel Processing Technology* 128: 499–508. doi: 10.1016/j.fuproc.2014.07.038
103. Sommersacher P, Kienzl N, Brunner T et al. (2016) Simultaneous Online Determination of S, Cl, K, Na, Zn, and Pb Release from a Single Particle during Biomass Combustion. Part 2: Results from Test Runs with Spruce and Straw Pellets. *Energy Fuels* 30(4): 3428–3440. doi: 10.1021/acs.energyfuels.5b02766
104. Thy P, Jenkins B, Grundvig S et al. (2006) High temperature elemental losses and mineralogical changes in common biomass ashes. *Fuel* 85(5-6): 783–795. doi: 10.1016/j.fuel.2005.08.020
105. Olsson JG, Jäglid U, Pettersson JBC et al. (1997) Alkali Metal Emission during Pyrolysis of Biomass. *Energy Fuels* 11(4): 779–784. doi: 10.1021/ef960096b
106. Davidsson KO, Stojkova BJ, Pettersson JBC (2002) Alkali Emission from Birchwood Particles during Rapid Pyrolysis. *Energy Fuels* 16(5): 1033–1039. doi: 10.1021/ef010257y
107. Enders M, Willenborg W, Albrecht J et al. (2000) Alkali retention in hot coal slag under controlled oxidizing gas atmospheres (air–CO<sub>2</sub>). *Fuel Processing Technology* 68(1): 57–73. doi: 10.1016/S0378-3820(00)00110-7
108. Thy P, Leshner CE, Jenkins BM (2000) Experimental determination of high-temperature elemental losses from biomass slag. *Fuel* 79(6): 693–700. doi: 10.1016/S0016-2361(99)00195-7
109. Wang Y, Wu H, Sárossy Z et al. (2017) Release and transformation of chlorine and potassium during pyrolysis of KCl doped biomass. *Fuel* 197: 422–432. doi: 10.1016/j.fuel.2017.02.046
110. Huron M, Oukala S, Lardière J et al. (2017) An extensive characterization of various treated waste wood for assessment of suitability with combustion process. *Fuel* 202: 118–128. doi: 10.1016/j.fuel.2017.04.025
111. Vassilev SV, Baxter D, Vassileva CG (2013) An overview of the behavior of biomass during combustion: Part I. Phase-mineral transformations of organic and inorganic matter. *Fuel* 112: 391–449. doi: 10.1016/j.fuel.2013.05.043
112. Glarborg P, Marshall P (2005) Mechanism and modeling of the formation of gaseous alkali sulfates. *Combustion and Flame* 141(1): 22–39. doi: 10.1016/j.combustflame.2004.08.014
113. Hindiyarti L, Frandsen F, Livbjerg H et al. (2008) An exploratory study of alkali sulfate aerosol formation during biomass combustion. *Fuel* 87(8): 1591–1600. doi: 10.1016/j.fuel.2007.09.001

114. Jørgensen TL, Livbjerg H, Glarborg P (2007) Homogeneous and heterogeneously catalyzed oxidation of SO<sub>2</sub>. Chemical Engineering Science 62(16): 4496–4499. doi: 10.1016/j.ces.2007.05.016
115. Wu H, Jespersen JB, Grell MN et al. (2013) Utilization of sulfate additives in biomass combustion: fundamental and modeling aspects. In: ETA-Florence Renewable Energies (ed) Proceedings of the 21st European Biomass Conference and Exhibition, pp 595–601
116. (2012) Verordnung über das Inverkehrbringen von Düngemitteln, Bodenhilfsstoffen, Kultursubstraten und Pflanzenhilfsmitteln: Düngemittelverordnung - DüMV
117. Patiño D, Crespo B, Porteiro J et al. (2016) Experimental analysis of fouling rates in two small-scale domestic boilers. Applied Thermal Engineering 100: 849–860. doi: 10.1016/j.applthermaleng.2016.02.112
118. Chapela S, Porteiro J, Garabatos M et al. (2019) CFD study of fouling phenomena in small-scale biomass boilers: Experimental validation with two different boilers. Renewable Energy 140: 552–562. doi: 10.1016/j.renene.2019.03.081